Volcanic risk ranking and regional mapping of the Central Volcanic Zone of the Andes

María-Paz Reyes-Hardy[1], Luigia Sara Di Maio[1], Lucia Dominguez[1], Corine Frischknecht[1], Sébastien Biass[1], Leticia Freitas Guimarães[2], Amiel Nieto-Torres[3], Manuela Elissondo[4], Gabriela Pedreros[5], Rigoberto Aguilar[6], Álvaro Amigo[5], Sebastián García[4], Pablo Forte[7], Costanza Bonadonna[1]

[1] Department of Earth Sciences, University of Geneva, Rue des Maraîchers 13, 1205 Geneva, Switzerland.
[2] Departamento de Geologia, Instituto de Geociências, Universidade Federal da Bahia, R. Barão de Jeremoabo, s/n - Ondina Salvador - BA, 40170-290, Brasil.
[3] Millennium Institute on Volcanic Risk Research - Ckelar Volcanoes, Avenida Angamos 0610, Antofagasta, Chile.
[4] Servicio Geológico Minero Argentino, SEGEMAR, Av. General Paz 5445 (colectora) Parque Tecnológico Miguelete Edificio 25. Piso 1 (Of 112) Buenos Aires, San Martin B1650KNA Argentina.
[5] Servicio Nacional de Geología y Minería, Red Nacional de Vigilancia Volcánica, Carlos Cardona Idarraga Rudecindo Ortega 03850, Temuco, Chile.
[6] Instituto Geológico Minero y Metalúrgico, Observatorio Vulcanológico del INGEMMET, Barrio Magisterial Nro. 2 B-16 Umacollo – Yanahuara, Arequipa, Perú.
[7] Observatorio Argentino de Vigilancia Volcánica (OAVV), SEGEMAR, CONICET, Av. Gral Paz 5445 Parque Tecnológico Miguelete. Edificio 25. Piso 1 (Of A1-03) Buenos Aires, San Martin B1650 WAB, Argentina.

Correspondence to: María-Paz Reyes-Hardy (maria-paz.reyeshardy@unige.ch)

Abstract. The Central Volcanic Zone of the Andes (CVZA) extends from southern Peru, through the Altiplano of Bolivia, to the Puna of northern Chile and Argentina, between latitudes 14-28°S of the Andean cordillera, with altitudes raising up to more than 4,000 m above sea level. Given the large number of active volcanoes in this area, which are often located close to both urban areas and critical infrastructure, prioritization of volcanic risk reduction strategies is crucial. The identification of hazardous active volcanoes is challenging due to the limited accessibility, scarce historical record, and the difficulty in identifying relative or absolute ages due to the extreme arid climate. Here, we identify the highest risk volcanoes combining complementary strategies: i) a regional mapping based on volcanic hazard parameters and surrounding density of elements at risk and ii) the application of the recently developed Volcanic Risk Ranking (VRR) methodology that integrates hazard, exposure and vulnerability as factors that increase risk, and resilience as a factor that reduces risk. We identified 59 active and potentially active volcanoes that not only include the volcanic centres with the most intense and frequent volcanic eruptions (e.g., El Misti and Ubinas volcanoes, Peru) but also the highest density of exposed elements (e.g., the cities of Arequipa and Mequegua, Peru). VRR was carried out for 19 out of the 59 volcanoes, active within the last 1,000 years or with unrest signs, highlighting those with the highest potential impact (i.e., Cerro Blanco in Argentina and Yucamane, Huaynaputina, Tutupaca, and Ticsani in Peru) and requiring risk mitigation actions to improve the capacity to face or overcome a disaster (e.g., volcanic hazard and risk/impact assessments, monitoring systems, educational activities, and implementation of early warning systems).

1 Introduction

The Central Volcanic Zone of the Andes (CVZA) is one of the four active volcanic zones in South America (Fig. 1). This zone between the latitudes 14-28°S comprises at least two volcanic segments controlled by a compressive subduction tectonics, with a diffuse boundary at 21°S between Isluga and Irruputuncu volcanoes. The northern CVZA segment, located in southern Peru and northernmost Chile-Bolivia, has major volcanoes aligned in a NW-SE direction and is characterized by significant historic magmatic eruptions. The southern segment within northern Chile, south-western Bolivia, and north-western Argentina on the other hand, has a more northerly trend comprising older edifices that have existed for up to circa a million years (e.g., Ollagüe, with a history going back as far as 800,000 years) and have longer repose periods (De Silva and Francis, 1991). The CVZA has an ongoing volcanism since the Late Eocene-Early Oligocene, comprising a wide diversity of activity patterns, volcanic landforms, products, and magma compositions (e.g., Bertin et al., 2022a; Grosse et al., 2018, 2022), including catastrophic sector collapses and a long record of voluminous silicic pyroclastic activity associated to potentially active giant ignimbrite centres and caldera systems with important implications for the safety of nearby communities (Stern, 2004).

The lack of knowledge due to scarce historical records and difficulty in identifying deposit ages together with its proximity to four international borders imply significant challenges for the CVZA, making it an area of interest for volcanic risk reduction. In fact, systematic studies of the CVZA only started in the 1970-80s, and increased during the last 20 years motivated by the implementation of new monitoring capabilities and research investments as a response to volcanic unrest in various areas, currently promoting cross-border collaborations (Aguilera et al., 2022; Forte et al., 2021). However, the characterization of hazardous active volcanoes is very challenging because of their limited accessibility. Several CVZA volcanoes are higher than 6,000 m above sea level (a.s.l), including Ojos del Salado, which is the highest volcanic summit of the world (Amigo, 2021). In addition, the extreme dry and arid conditions further complicate detailed studies of these volcanoes. As an example, the determination of the relative ages through morphology is hampered by the very low erosion rates making difficult the distinction between old and fresh volcanic features. Existing radiocarbon techniques are also limited because deposits usually lack or contain only small amounts of organic carbon (Gillespie et al., 1991; De Silva and Francis, 1991). Finally, the CVZA volcanoes are located within 25 km of international borders, in between Argentina, Chile, Bolivia or Peru. Andean communities have interacted with these volcanic features for more than 11,000 years well before border delineation (Ramos Chocobar and Tironi, 2022; Loyola et al., 2022). However, the current division of borders increases the challenges of volcanic risk management since each country has multiple strategies, resources, sovereignty and intrinsic socio-economic and political conditions playing a key role when facing natural risks (e.g., Donovan and Oppenheimer, 2019; Petit-Breuilh Sepúlveda, 2016; Romero and Albornoz, 2013).

One of the major difficulties within the CVZA lies in the identification of active hazardous volcanoes. Although various nomenclatures have been proposed to describe the state of a volcano (e.g., Szakács, 1994; Auker et al., 2015), here we follow

Szakács definition, also in agreement with the Geological Services of Argentina (SEGEMAR), Chile (SERNAGEOMIN), and Peru (INGEMMET). According to Szakács (1994) "active volcano" and "extinct volcano" are mutually exclusive terms. Active volcanoes are geologically active when they had at least one eruption in the Holocene period, and they can be subdivided into "erupting" and "dormant" types based on their current state of activity. Extinct volcanoes have not had eruptions during the Holocene and can be classified as "young" or "old" using criteria such as the extent of erosion or geochronological age. The term "potentially active" is reserved for those fresh-looking volcanoes lacking both documented eruptions and reliable absolute ages. "Potentially active" volcanoes could be defined as "active-dormant" or "extinct-young" volcanoes as more information becomes available (Szakács, 1994). Alternatively, in absence of data of eruptions during the Holocene, a volcano can be considered "potentially active" when it presents visible signs of unrest activity such as degassing, seismicity or ground deformation (e.g., Simkin and Siebert, 1994; Ewert et al., 2005; Ewert, 2007; Lara et al., 2011). As a result, in this study we analyse a total of 59 volcanoes, 25 active Holocene volcanoes and 34 potentially active volcanoes having fresh volcanic morphology or records of at least one sign of unrest (i.e., seismicity, deformation or degassing).

Volcanic rankings have been used to identify threatening volcanoes, notably based on the strategy proposed by Ewert et al. (1998; 2005; 2007), that combines hazard (the destructive natural phenomena produced by a volcano) and exposure (people and property at risk from the hazards) parameters. Based on this methodology, three of the four countries of the CVZA have already produced a relative volcanic threat ranking considering the whole country (e.g., Macedo et al., 2016; Lara et al., 2006; SERNAGEOMIN, 2020, 2023; Elissondo et al., 2016; García et al., 2018; Elissondo and Farías, 2024). Peru ranked 16 volcanoes with four levels of threat, from very low to very high (Macedo et al., 2016). Chile recently updated its volcanic ranking of 87 active and potentially active volcanoes based on 13 hazard and 12 exposure parameters (SERNAGEOMIN, 2023). A new volcanic risk ranking for Argentina was also recently published with 38 active and potentially active volcanoes based on 15 hazard and 10 exposure parameters (Elissondo and Farías, 2024). From these rankings only 26 (Chilean ranking) and 22 (Argentinian ranking) volcanic centres, as well as all 16 volcanoes of the Peruvian ranking, are part of the CVZA. However, many active and potentially active volcanoes of the CVZA and their eruptive histories remain understudied. Recently, a new Volcanic Risk Ranking (VRR) methodology was proposed, expanding the work of Ewert et al. (1998; 2005), by integrating additional factors that can influence the risk level, i.e., vulnerability, as characteristics of the elements at risk that can increase the susceptibility to the impact of a natural hazard; and resilience, as the system's ability to adapt to changes, overcome disturbances and maintain functionality from the effects of a hazard (Nieto-Torres et al., 2021; Guimarães et al., 2021). This new VRR methodology was tested on Mexican volcanoes with activity recorded in the last 10,000 and 1,000 years (Nieto-Torres et al., 2021) and applied to Latin American volcanoes with activity recorded in the last 1,000 years (Guimarães et al., 2021).

In this study, we identify the volcanoes of the CVZA with the highest potential impact based on two complementary strategies: i) the regional mapping of hazard parameters and elements at risk for a total of 59 active and potentially active volcanoes, and

ii) the VRR methodology proposed by Nieto-Torres et al., (2021) for 19 volcanoes considered more likely to have an eruption in the future. Our study underlines two main aspects. First, it demonstrates the challenges of regional risk assessment, especially for cross-boundary volcanoes managed by multiple institutions and associated with different geographical contexts. Second, the combination of multiple risk factors (hazard, exposure, vulnerability and resilience) provides fundamental insights for risk management. Indeed, the regional mapping and regional VRR provides the opportunity to consider transboundary volcanoes that are often neglected by local authorities, typically more focused on active volcanoes with short repose intervals, or those that lack any resilience measures.

2 Geological setting of the CVZA

The Andean Cordillera started building during the late Paleozoic, characterized by an important magmatism associated with the beginning of the subduction in the Pacific margin (Ramos and Aleman, 2000; Tilling, 2009), while its evolution began in the earliest Jurassic in association with the opening of the Southern Atlantic Ocean (Stern, 2004). The most significant events in the evolution of the Andes occurred after the breakup of the Farallon plate into the Cocos and Nazca plates in the Late Oligocene ($\sim 27\pm2$ Ma) that caused changes in subduction geometry, and accelerated crustal shortening, thickening and uplift in the Northern and Central Andes (Jaillard et al., 2000; Ramos and Aleman, 2000; Jordan et al., 1983; Sempere et al., 1990; Hall et al., 2008). The resulting increase in convergence rates drove the magmatic activity nearly all along the Andes (Stern, 2004). Although many of the main features of the Andes were formed during the Miocene, Quaternary deformation significantly modified the topography, controlled the location of active volcanoes and thus the distinction among small arc segments within the main volcanic zones (Stern, 2004). A total of 204 out of the 1,500 active volcanoes during the Holocene worldwide are part of the Andes, but their distribution is not continuous along the Andean margin (Tilling, 2009; GVP, 2023a). Four main zones can be identified (Fig. 1): the Northern Volcanic Zone of the Andes (NVZA) from Colombia to Ecuador; the Central Volcanic Zone of the Andes (CVZA) along southern Peru, northern Chile, south-western Bolivia, and north-western Argentina; the Southern Volcanic Zone of the Andes (SVZA) extending from central to southern Chile and Argentina; and finally, the Austral Volcanic Zone of the Andes (AVZA), along the southernmost region of the continent. These segments are separated from each other by volcanically inactive gaps that may be a result of the subduction of the Nazca and Juan Fernandez ridges, which is an important factor controlling the geometry of Andean flat-slabs (e.g., Barazangi and Isacks, 1976; Thorpe et al., 1984; Pilger, 1984; Stern, 2004; Tilling, 2009; Kay and Coira, 2009).

The CVZA, the aim of this study, is located between latitudes 14° and 28°S of the Andean cordillera, between the Peruvian and Pampean flat-slab segments (Fig. 1). All the volcanoes in this zone are above 3,500 m a.s.l., constituting a high, remote, and exceptionally arid region (De Silva and Francis, 1991). It is formed by the subduction of the Nazca Plate below the South American Plate at a convergence rate of 7-9 cm per year and an angle of 30° to the trench (Cahill and Isacks, 1992; Hayes et al., 2018; Gianni et al., 2019). The continental crust in the CVZA reaches a thickness of up to 65-70 km (James, 1971; Van

der Meijde et al., 2013), composed of Cenozoic volcanic rocks overlying a 2,000 Ma basement in the northern part and Late
135   Precambrian-to-Paleozoic substrate in the southern segment (Walker et al., 2013). Andesites, dacites and rhyolites are the
dominant rock composition in the CVZA, although basaltic andesites and occasional basalts occur. The most relevant volcanic
hazards of the Central Andean volcanoes include tephra fallout, pyroclastic density currents, ballistics, lava flows and lava
domes, debris flows, and lahars (Bertin et al., 2022a).

140 **Figure 1: Location map showing the Northern Volcanic Zone of the Andes (NVZA; grey triangles), Central Volcanic Zone of the Andes (CVZA; yellow triangles), Southern Volcanic Zone of the Andes (SVZA; blue triangles), and Austral Volcanic Zone of the Andes (AVZA; green triangles). Modified from Stern (2004). Layer Sources: Esri, USGS, NOAA.**

3 Methodology

This study includes the analysis of volcanoes in the four countries prone to be impacted by future volcanic activity of the
145 CVZA (i.e., Peru, Bolivia, Argentina and Chile). Four main steps were carried out: 1) compilation of active and potentially active volcanoes of the CVZA based on the existing catalogues of De Silva and Francis (1991), GVP (2013), Macedo et al. (2016), SERNAGEOMIN (2023), Elissondo and Farías (2024) and Aguilera et al. (2022), including a detailed review of hazard and resilience parameters, available in Reyes-Hardy et al., (2023); 2) identification of elements at risk (e.g., population, transportation and critical facilities); 3) regional mapping that includes both volcanic hazard features and surrounding elements
150 at risk for all the 59 identified active and potentially active volcanoes of the CVZA; 4) application of the VRR methodology (Nieto-Torres et al., 2021) to identify the highest risk volcanoes of the CVZA based on the estimation and scoring of hazard, exposure, vulnerability and resilience parameters. This last step focused on the 19 volcanoes having shown volcanic activity during the past 1,000 years or records of three signs of unrest (i.e., seismicity, ground deformation and degassing).

3.1 Identification of active and potentially active volcanoes of the CVZA

155 The first challenge in ranking the risk amongst volcanoes in a specific area is the selection of volcanoes to consider. Since geochronological data or preserved historical records are largely absent in the CVZA, the term "potentially active" has been widely used to account for this lack of data. This has led to discrepancies in the CVZA volcano count evidenced in the number of potentially active eruptive centres identified by De Silva and Francis (1991) (n=73), the Global Volcanism Program database (n=67; GVP, 2013), as well as within different catalogues accounting for CVZA volcanoes (i.e., Elissondo et al., 2016;
160 SERNAGEOMIN, 2020; Aguilera et al., 2022; Macedo et al., 2016; SERNAGEOMIN, 2023; Elissondo and Farías, 2024). The first step of our study was the compilation of the active and potentially active volcanoes of the CVZA based on a comprehensive analysis of six catalogues in collaboration with SEGEMAR, SERNAGEOMIN, and INGEMMET, combined with their own updated volcanic risk rankings relative for each country (i.e., Argentina, Elissondo and Farías, 2024; Peru, Macedo et al., 2016; and Chile, SERNAGEOMIN, 2023). A total of 59 volcanic centres have been identified as active or
165 potentially active, of which 50 have Holocene and 9 Pleistocene activity (Table 1). In terms of geographical distribution, 12 volcanoes are located in Chile, nine in Argentina, 13 on the Chile-Argentina border, seven on the Chile-Bolivia border, two in Bolivia and 16 in Peru. In terms of types of volcanoes, 34 are stratovolcanoes, 15 are volcanic complexes, three are volcanic fields, one is a pyroclastic cone, four are dome complexes, one is a maar and one is a caldera (Supplementary material 1). Among volcanoes with Holocene activity, 16 volcanoes had at least one eruption in the last 1,000 years. In addition, three
170 volcanoes (one with Pleistocene and two with Holocene activity) with eruptions older than 1,000 years, show records of all three signs of unrest (i.e., seismicity, ground deformation and degassing). The complexity associated with the definition of active and potentially active volcanoes of the CVZA highlights the challenging characterization of volcanoes in this area,

6

including those with long repose intervals and/or poor constraints on their eruptive record. Although our volcano list is the best agreement of active and potentially active volcanoes of the CVZA, such a list can change depending on future knowledge

175 of this zone including geochronology and monitoring studies.

Table 1. List of the active and potentially active volcanoes of the CVZA (extracted from Supplementary material 1). C.: Cerro, N.: Nevado (s), Pe: Peru, Ch: Chile, Bo: Bolivia, Ar: Argentina, H: Holocene, Pl: Pleistocene, DC: Dome complex, PC: Pyroclastic cone, ST: Stratovolcano, VF: Volcanic field, VC: Volcanic complex, S: Seismic unrest records, G: Ground deformation records, D:
180 **Fumarolic/magmatic degassing records, U: Unknown, and ND: No data. Notice that volcanoes with last eruption during the past 1,000 years and/or presenting records of all three signs of unrest are in bold.**

N°	Volcano name	Latitude	Longitude	Country	Type	Age	Last eruption	Signs of unrest	N° Holocene eruptions	Max VEI
1	Quimsachata	14.13°S	71.36°W	Pe	DC	H[*]	4450 BCE[*]	No	1	ND
2	C. Auquihuato	15.07°S	73.18°W	Pe	PC	H[*,90]	U[*]	G[72]	ND	ND
3	Sara Sara	15.33°S	73.45°W	Pe	ST	Pl[*,1]	14000 BCE[65]	No	0[1]	ND[1]
4	**Andahua**	15.42°S	72.33°W	Pe	VF	H[*]	**1490 CE[*]**	D[90]	4 (3)	ND
5	Coropuna	15.52°S	72.65°W	Pe	ST	H[*]	~700 BP[65]	D[73]	ND	ND
6	Huambo	15.78°S	72.08°W	Pe	VF	H[*]	700 BCE[*]	No	1 (1)	ND
7	**Sabancaya**	15.78°S	71.85°W	Pe	ST	H[*]	**2016 – present[65]**	**S[76], G[74,75], D[77]**	14 (12)	3
8	Chachani	16.19°S	71.53°W	Pe	VC	Pl[2]	56 000 ya[65]	S[78], D[79]	0	ND
9	**El Misti**	16.29°S	71.40°W	Pe	ST	H[*]	**1440 - 1470 CE[65]**	S[80], D[81]	22 (15)	5[69]
10	**Ubinas**	16.35°S	70.90°W	Pe	ST	H[*]	**2019 CE[*]**	**S[82], G[84], D[83]**	26 (23)	5
11	**Huaynaputina**	16.60°S	70.85°W	Pe	ST	H[*]	**1600 CE[*]**	D[85]	2 (2)	6
12	**Ticsani**	16.75°S	70.59°W	Pe	ST	H[*]	**1800 CE[*]**	**S[88], G[86,87], D[89]**	1 (1)	2-3[70]
13	**Tutupaca**	17.02°S	70.37°W	Pe	ST	H[*]	**1802 CE[*]**	D[8]	5 (2)	4
14	**Yucamane**	17.18°S	70.19°W	Pe	ST	H[*]	**1787 CE[66]**	D[9,10]	1 (1)	5
15	Purupuruni	17.32°S	69.90°W	Pe	DC	H[3]	Pl[*]	No	ND	ND
16	Casiri	17.47°S	69.81°W	Pe	ST	H[*]	2600 ± 400 BP[65]	D[11]	ND	ND
17	Tacora	17.72°S	69.77°W	Ch	ST	H[*]	U[*]	S[12,13], D[14,15,16]	2 (0)	ND
18	Taapaca	18.10°S	69.50°W	Ch	VC	H[*]	320 BCE[*]	(G, D)[14]	8 (8)	ND
19	**Parinacota**	18.16°S	69.14°W	Ch-Bo	ST	H[*]	**1803 CE[67]**	S[17]	38[67] (6)	4[71]
20	**Guallatiri**	18.42°S	69.09°W	Ch	ST	H[*]	**1960 CE[*]**	S[18,19], D[20,21,22]	6 (4)	2
21	Tata Sabaya	19.13°S	68.53°W	Bo	ST	H[*]	U[*]	No	ND	ND
22	**Isluga**	19.15°S	68.83°W	Ch	ST	H[*]	**1913 CE[*]**	S[23], D[5,14,24]	8 (7)	2
23	**Irruputuncu**	20.73°S	68.55°W	Ch-Bo	ST	H[*]	**1995 CE[*]**	(S, D)[14,18]	2 (1)	2
24	Olca-Paruma	20.93°S	68.41°W	Ch-Bo	VC	H[*]	U[*]	D[14,25]	1 (0)	ND
25	Aucanquilcha	21.22°S	68.47°W	Ch	ST	Pl[*]	Pl[*]	D[5]	0	ND

7

#	Name	Lat	Long	Country	Type			References		
26	Ollagüe	21.30°S	68.18°W	Ch-Bo	ST	Pl*	Pl*	(S, D)[14,18,86]	0	ND
27	C. del Azufre	21.78°S	68.23°W	Ch	VC	H*	U*	G[23,45,74], D[26]	ND	ND
28	**San Pedro**	21.88°S	68.39°W	Ch	ST	H*	**1960 CE***	D[14]	10 (6)	2
29	**Uturuncu**	22.27°S	67.18°W	Bo	ST	Pl*	Pl*	S[30], G[74,27,28,29,32,33,34], D[31]	0	ND
30	**Putana**	22.55°S	67.85°W	Ch-Bo	ST	H*	**1810 CE***	S[25,28,18], G[28], D[25,28,18]	2 (1)	2
31	Escalante-Sairecabur	22.72°S	67.89°W	Ch-Bo	VC	H*	U*	No	ND	ND
32	Licancabur	22.83°S	67.88°W	Ch-Bo	ST	H*	U*	No	ND	ND
33	Acamarachi	23.29°S	67.61°W	Ch	ST	H*	U*	No	ND	ND
34	**Lascar**	23.37°S	67.73°W	Ch	ST	H*	**2023 CE****	S[36], G[35], D[37,38,39,40]	37 (32)**	4
35	Chiliques	23.58°S	67.70°W	Ch	VC	H*	U*	D[41]	ND	ND
36	Alitar	23.80°S	67.39°W	Ch	Maar	Pl[4]	Pl[4]	D[20]	0	ND
37	Puntas Negras	23.44°S	67.32°W	Ch	VC	H[5]	ND	No	ND	ND
38	Tuzgle	24.05°S	66.48°W	Ar	ST	H*	U*	No	ND	ND
39	Aracar	24.29°S	67.78°W	Ar	ST	H*	U*	No	1 (0)	2
40	Socompa	24.39°S	68.24°W	Ch-Ar	ST	H*	5250 BCE*	G[42,43], D[5,24,14,44]	1 (1)	ND
41	Arizaro	24.45°S	68.023°W	Ar	VF	H[6]	80,000 ± 60,000 BP[68]	No	ND	ND
42	**Llullaillaco**	24.72°S	68.53°W	Ch-Ar	ST	H*	**1877 CE***	No	3 (3)	2
43	Escorial	25.08°S	68.36°W	Ch-Ar	ST	H*	U*	No	ND	ND
44	**Lastarria**	25.16°S	68.50°W	Ch-Ar	ST	H*	U*	S[14,18,51], G[74,45,46,47,48,49,50], D[20,22,52,53,54,55]	ND	ND
45	Cordón del Azufre	25.33°S	68.52°W	Ch-Ar	VC	H*	U*	No	ND	ND
46	C. Bayo	25.41°S	68.58°W	Ch-Ar	VC	H*	U*	G[23,45,74]	ND	ND
47	Antofagasta	26.12°S	67.40°W	Ar	VC	H*	U*	No	ND	ND
48	Sierra Nevada	26.48°S	68.58°W	Ch-Ar	VC	H*	U*	No	ND	ND
49	Cueros de Purulla	26.55°S	67.82°W	Ar	DC	Pl[7]	ND	No	0	ND
50	Peinado	26.62°S	68.11°W	Ar	ST	H*	U*	No	ND	ND
51	C. El Cóndor	26.63°S	68.36°W	Ar	ST	H*	U*	No	ND	ND
52	**C. Blanco**	26.78°S	67.76°W	Ar	Caldera	H*	2300 BCE*	S[60], G[74,23,28,56,57,58,59], D[56,61,62]	1 (1)	7
53	Falso Azufre	26.80°S	68.37°W	Ch-Ar	VC	H*	U*	No	ND	ND
54	N. de Incahuasi	27.03°S	68.29°W	Ch-Ar	VC	H*	U*	No	ND	ND
55	El Fraile	27.04°S	68.37°W	Ch-Ar	DC	Pl[7]	ND	D[63]	0	ND
56	N. Tres Cruces	27.08°S	68.80°W	Ch-Ar	ST	Pl*	Pl*	No	0	ND
57	El Solo	27.10°S	68.71°W	Ch-Ar	ST	H*	U*	No	ND	ND
58	N. Ojos del Salado	27.10°S	68.54°W	Ch-Ar	VC	H*	750 CE*	D[86,64]	2 (1)	1

| 59 | C. Tipas | 27.19°S | 68.56°W | Ar | VC | H[*] | U[*] | No | ND | ND |

[*] GVP (2013), [**] GVP (2023a, b), [1]Rivera et al. (2020), [2]Aguilar et al. (2022), [3]Bromley et al. (2019), [4]Amigo et al. (2012), [5]De Silva and Francis (1991), [6]Viramonte et al. (1984), [7]Bertin (2022), [8]Mariño et al. (2019), [9]Fídel and Huamaní (2001), [10]Cruz et al. (2010), [11]Cruz et al. (2020), [12]Clavero et al. (2006), [13]Pavez et al. (2019), [14]Lara et al. (2011), [15]Capaccioni et al. (2011), [16]Contreras (2013), [17]REAV Parinacota (2020), [18]Pritchard et al. (2014), [19]SERNAGEOMIN (2021), [20]Aguilera (2008), [21]Inostroza et al. (2020a), [22]Inostroza et al. (2020b), [23]Pritchard and Simons (2004), [24]González-Ferrán (1995), [25]Tassi et al. (2011), [26]Aguilera et al. (2020), [27]Fialko and Pearse (2012), [28]Henderson and Pritchard (2013), [29]Hickey et al. (2013), [30]Jay et al. (2012), [31]Sparks et al. (2008), [32]Gottsmann et al. (2017), [33]Henderson et al. (2017), [34]Pritchard et al. (2018), [35]Pavez et al. (2006), [36]Gaete et al. (2019), [37]Matthews et al. (1997), [38]Aguilera et al. (2006), [39]Tassi et al. (2009), [40]Bredemeyer et al. (2018), [41]Pieri and Abrams (2004), [42]Liu et al. (2022), [43]Liu et al. (2023), [44]Seggiaro and Apaza (2018), [45]Froger et al. (2007), [46]Ruch et al. (2008), [47]Ruch et al. (2009), [48]Anderssohn et al. (2009), [49]Ruch and Walter (2010), [50]Budach et al. (2011), [51]Spica et al. (2012), [52]Naranjo (1985), [53]Aguilera et al. (2012), [54]Aguilera et al. (2016), [55]Robidoux et al. (2020), [56]Viramonte et al. (2005), [57]Brunori et al. (2013), [58]Vélez et al. (2021), [59]Báez et al. (2015), [60]Mulcahy et al. (2010), [61]Chiodi et al. (2019), [62]Lamberti et al. (2021), [63]Salas (2022, pers. comm.), [64]Gardeweg et al. (1998), [65]IGP (2021), [66]OVI (2021), [67]Bertin et al. (2022b), [68]Schoenbohm and Carrapa (2015), [69]Harpel et al. (2011), [70]Cruz (2020), [71]Clavero et al. (2004), [72]Morales Rivera et al. (2016), [73]Ramos (2019), [74]Pritchard and Simons (2002), [75]Jay et al. (2015), [76]Samaniego et al. (2016), [77]BGVN (2021), [78]Centeno et al. (2013), [79]Gałaś et al. (2014), [80]Sandri et al. (2014), [81]Thouret et al. (2001), [82]Del Carpio and Torres (2020), [83]Rivera et al. (2010), [84]Apaza et al. (2021), [85]Antayhua et al. (2013), [86]Jay et al. (2013), [87]Gonzáles et al. (2006), [88]Holtkamp et al. (2011), [89]Byrdina et al. (2013), [90]Macedo et al. (2016). Notice that if not indicated otherwise, the "Max VEI" and "N° Holocene eruptions" values correspond to the maximum VEI, and the number of eruptions and confirmed eruptions (in parenthesis) during the Holocene according to GVP (2013, 2023a).

3.2 Elements at risk

In this study, the elements at risk include population, residential buildings, critical infrastructure (e.g., transportation, power, water and telecommunication supply networks), emergency facilities (e.g., police and fire stations), critical facilities (e.g., government offices, schools), and economic activities (e.g., parks and protected areas, mines, salt pans, farmlands, industrial areas). Each dataset is country-specific, favouring official sources (e.g., ministries, national geographic institutes, national observatories, statistical institutes). Open-source datasets (e.g., HOT, 2020) were used to complete missing official information. All details and sources of elements at risk are available in Supplementary material 2.

Concerning the population, density data are provided by WorldPop - Open Spatial Demographic Data and Research (WorldPop, 2018). Worldpop data used in this study represent the spatial distribution of resident population density in 2020 per grid-cell (inhabitants per km^2), and they are provided at country level (i.e., Peru, Bolivia, Argentina, and Chile), with a resolution of 30 arc seconds (approximately 1 km at the equator). Obtained from the so-called top-down unconstrained modelling; this method misplaces the population in some locations showing the presence of people in uninhabited areas (WorldPop, 2023). A validation with satellite images was used to correct and reclassify the discrepancies with non-zero population to the range of 0-0.1 inhabitants per km^2. This data correction allowed us to obtain results of population density that were more consistent with the density and distribution of populated centres (see Supplementary material 2). National

censuses were used to extract socio-economic data required to constrain the VRR exposure parameters (IGN, 2010; INDEC, 2010; INE, 2012, 2017a, 2017b; INEI, 2017; IDE, 2021; ONEMI, 2021a, 2021b).

Transportation includes: i) road network, ii) rail network, iii) airports and air routes, iv) harbours, v) ferry terminals along rivers and lakes, and vi) border crossing check posts (Supplementary material 2). A taxonomy homogenization of the road network was required to reclassify in five categories as described in Table 2. In the case of rural paths, only connecting routes between rural centres (i.e., important exposed element in the CVZA) have been considered. There are no distinctions between railways (e.g., passenger transport, freight, tourist lines) and all lines and train stations have been included. Ferry terminals along rivers and lakes are also included. Given the geographical characteristics of the countries analysed, particularly the hydrological characteristics, these facilities are essential.

Table 2. Standardization of road classification in Argentina, Bolivia, Chile and Peru.

Road type	ARGENTINA	BOLIVIA	CHILE	PERU
Primary Road	Red Vial Primaria	Red Vial Fundamental (RVF)	Ruta Internacional, Ruta Nacional	Red Vial Nacional
Secondary Road	Red Vial Secundaria	Redes Departamentales	Caminos Regionales Principales	Red Vial Departamental
Tertiary Road	Red Vial Terciaria	Redes Municipales	Caminos Regionales Provinciales	Red Vial Vecinal
Urban Road	Red Vial Urbana	Local network	Caminos Regionales Comunales y de Acceso	Local network
Rural Paths	Senda Rural	Rural Paths	Vías Rurales	Rural Paths

Facilities are «all manmade structures or other improvements that, because of their function, size, service area, or uniqueness, have the potential to cause serious bodily harm, extensive property damage, or disruption of vital socio-economic activities if they are destroyed, damaged, or if their functionality is impaired» (FEMA 2007). Facilities considered are divided into two groups: i) emergency facilities (e.g., civil protection headquarters, police stations, fire stations; see Supplementary Material 2) and ii) critical facilities. The first group consists of essential services to public safety and health; the second one includes strategic structures for social and economic sectors.

3.3 Regional mapping

The regional mapping consists in combining volcanic hazard features and elements at risk, representing a first-order analysis of volcanoes that could have a potential impact in the region. In terms of hazard, the number of eruptions and the maximum VEI during the Holocene have been represented as well as the age of their last eruption. In terms of elements at risk, density maps were produced for population, transportation and critical and emergency facilities at a 1 km spatial resolution. For the

10

population density map, we classified population density in four ranges (i.e., 0-1, 1-10, 10-100, and >100 inhabitants per km^2). The transport density combines point features expressed in the number of structures per km^2 (i.e., train stations, airports, harbours, and border crossings) and linear features expressed in kilometres of infrastructure per km^2 (i.e., road network, railways, and air routes). Critical and emergency facilities are expressed as number of facilities per km^2. Separate layers of hazard and density of elements at risk are presented in Supplementary Material 3.

3.4 Volcanic Risk Ranking

The identification of the volcanic systems with the highest potential risk was performed using the VRR methodology introduced by Nieto-Torres et al. (2021) and applied to Latin American volcanoes by Guimarães et al. (2021). The VRR step was carried out for the 19 active and potentially active volcanoes identified based on their activity during the past 1,000 years or records of three signs of unrest (i.e., seismicity, ground deformation and degassing). We apply the VRR-0 (2 factors), VRR-1 (3 factors) and VRR-2 (4 factors) strategies of Nieto-Torres et al. (2021):

$$VRR - 0 \ (threat) = Hazard \times Exposure \ , \tag{1}$$

$$VRR - 1 = Hazard \times Exposure \ \times Vulnerability \ , \tag{2}$$

$$VRR - 2 = (Hazard \times Exposure \times Vulnerability)/(Resilience + 1) \ , \tag{3}$$

Vulnerability considers 4 dimensions (physical, systemic, social, and economic), while resilience includes 2 dimensions (mitigation measures and response) (Nieto-Torres et al., 2021). As VRR – 2 is a ratio, the resilience factor is mathematically corrected with the value of 1, after the aggregation of resilience parameters and before normalization, to obtain a VRR result even for cases where the resilience factor is equal to zero (Nieto-Torres et al., 2021).

There are 9 hazard parameters, 9 exposure parameters, 10 vulnerability parameters and 13 resilience parameters (details in Supplementary material 4). The scores previously assigned for each parameter by Guimarães et al. (2021) have been updated as more recent information became available (e.g., historical eruption of Parinacota volcano, increasing population density, telecommunication facilities; and updated multiple economic activities). Each risk factor (i.e., hazard, vulnerability, exposure and resilience) was normalized to the maximum possible score and multiplied by the value of 10, to guarantee the same weight. Therefore, the scores were normalized based on the maximum possible value for each of the evaluated factors (19 for hazard, 48 for exposure, 95 for vulnerability, and 18 for resilience). The maximum hazard score represents the highest intensity of each volcanic process; the maximum exposure score is the largest quantity of assets prone to be affected; and the maximum vulnerability score, represents the highest level of susceptibility to damage or loss. In contrast, the maximum resilience score represents the maximum level of capacity to face or overcome a disaster (Nieto-Torres et al., 2021).

11

4. Results

4.1 Regional mapping of the CVZA

270 The regional maps resulting from the combination of the 59 CVZA active and potentially active volcanoes with the density maps of population, transportation and facilities are shown in Fig. 2, 3 and 4, respectively. Five zones with more than 100 inhabitants per km^2 are identified close to volcanoes showing various eruptive frequencies and VEIs (Fig. 2). The first zone includes the city of Arequipa (Peru), with El Misti and Ubinas volcanoes standing out due to their high eruptive frequency (22 and 26 Holocene eruptions, respectively). The second zone comprises the city of Moquegua (Peru), close to Huaynaputina

275 (maximum VEI of 6), and Ticsani, Tutupaca and Yucamane volcanoes (VEI 2-3, 4 and 5, respectively). The third zone includes the city of Tacna (Peru) close to Tacora, Casiri, Purupuruni and Yucamane volcanoes with the last having a maximum VEI of 5. The fourth zone comprises the city of Calama (Chile) close to San Pedro volcano with a medium eruptive frequency (10 Holocene eruptions). The fifth zone corresponds to the mining stations "Estación Zaldivar" and "Mina Escondida", close to Llullaillaco volcano with low eruptive frequency and VEI (3 Holocene eruptions and VEI 2). Additionally, in the southern

280 zone of the CVZA there is Cerro Blanco volcano (Argentina), whose eruption is among the largest volcanic eruptions of the Holocene globally (VEI 7; Fernandez-Turiel et al., 2019). Even though Cerro Blanco is not close to inhabited areas with more than 100 inhabitants per km^2, there are important populated localities within 100 km around the volcano: Antofagasta de la Sierra (730 inhabitants), Palo Blanco (992 inhabitants), Corral Quemado (1200 inhabitants), Punta del Agua (172 inhabitants) and Antinaco (105 inhabitants) (see Supplementary material 2).

285

Six areas can be identified based on the highest density distribution of transport infrastructure (Fig. 3): 1) the cities of Arequipa, Moquegua, and Tacna (Peru), close to the volcanoes Sabancaya, El Misti, Ubinas, Huaynaputina, Ticsani, Tutupaca, Yucamane, Purupuruni, Casiri and Tacora. 2) two border crossings, i.e., the triple point (geographical point where the borders of Peru, Bolivia and Chile meet) and Colchane customs post (one of the border crossings between Bolivia and Chile), close to

290 the volcanoes Casiri, Tacora and Taapaca (with no confirmed VEI); and Tata Sabaya and Isluga respectively, with no information and a medium eruptive frequency (8 Holocene eruptions) and VEI (2), respectively. 3) the Collahuasi mining district, representing one of the largest copper reserves in Chile and in the world, close to Irruputuncu and Olca-Paruma volcanoes, which have a low number of Holocene eruptions and low VEI (2) or not confirmed. 4) Calama city and San Pedro volcano, with a medium eruptive frequency (10 Holocene eruptions) and low VEI (2). 5) San Pedro de Atacama town, a

295 popular tourist destination in Antofagasta region (Chile) close to Putana, Escalante-Sairecabur and Licancabur volcanoes (the first having 2 Holocene eruptions and VEI 2, and the last two with no information available); and 6) Sociedad Química y Minera de Chile (SQM), the world's biggest lithium producer close to Lascar volcano, which has a high eruptive frequency (37 Holocene eruptions) and maximum VEI (4). Finally, the area with the highest amount of emergency and critical facilities per km^2 is concentrated in Arequipa city (Peru) close to Sabancaya, El Misti and Ubinas volcanoes (Fig. 4).
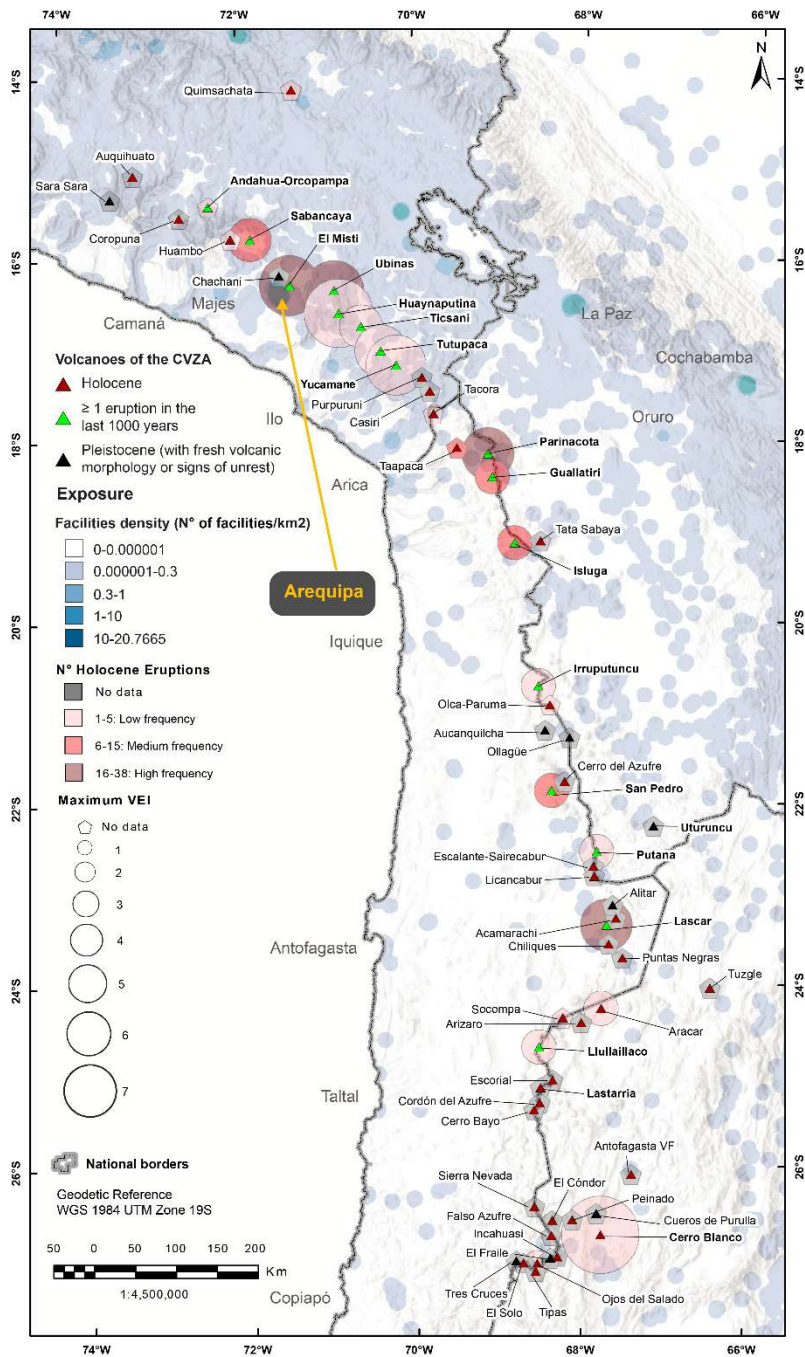
300

12
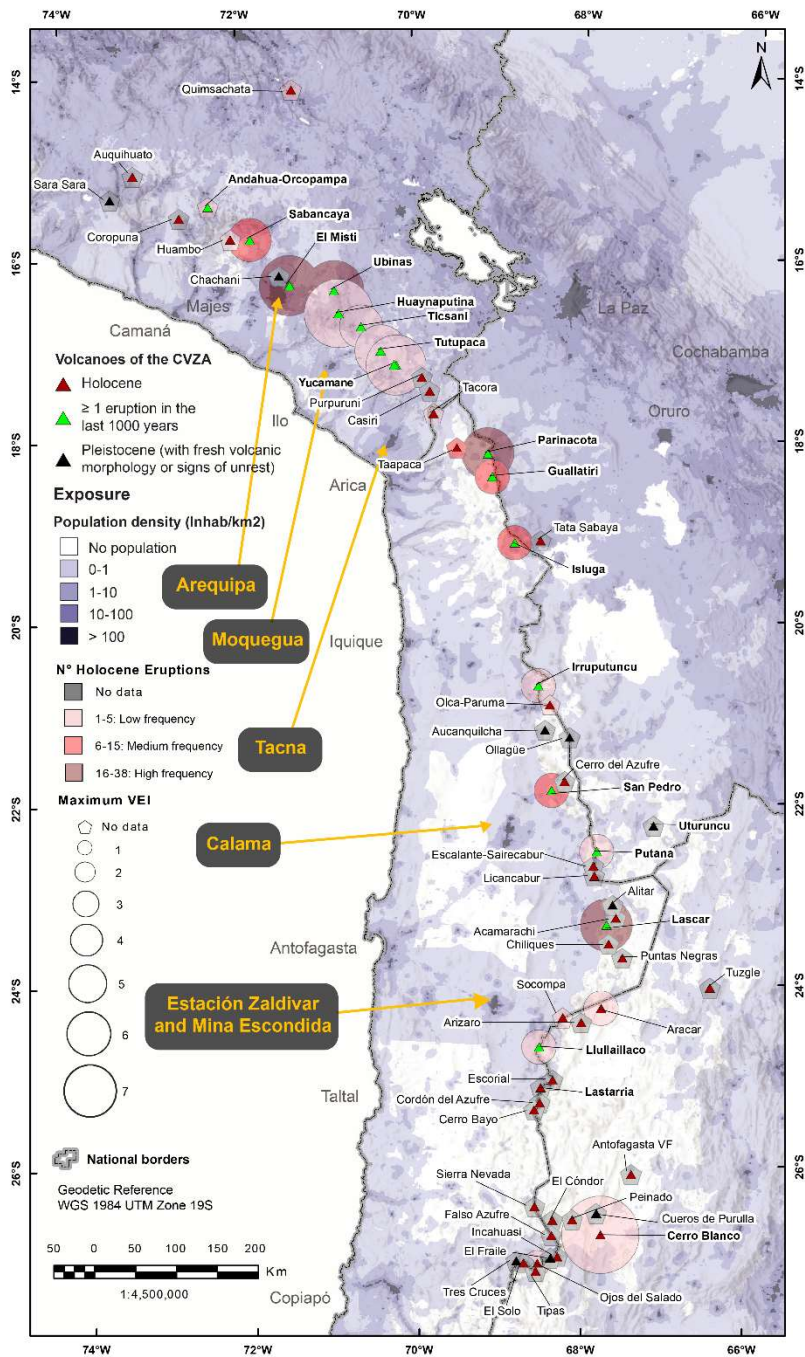
Figure 2: Regional map including the total CVZA active and potentially active volcanoes and population density, with the Maximum VEI during the Holocene and the number of Holocene eruptions of the CVZA volcanoes superimposed. Notice that the 19 volcanoes considered for the VRR analysis are in bold. Layer Sources: Esri, USGS, NOAA.
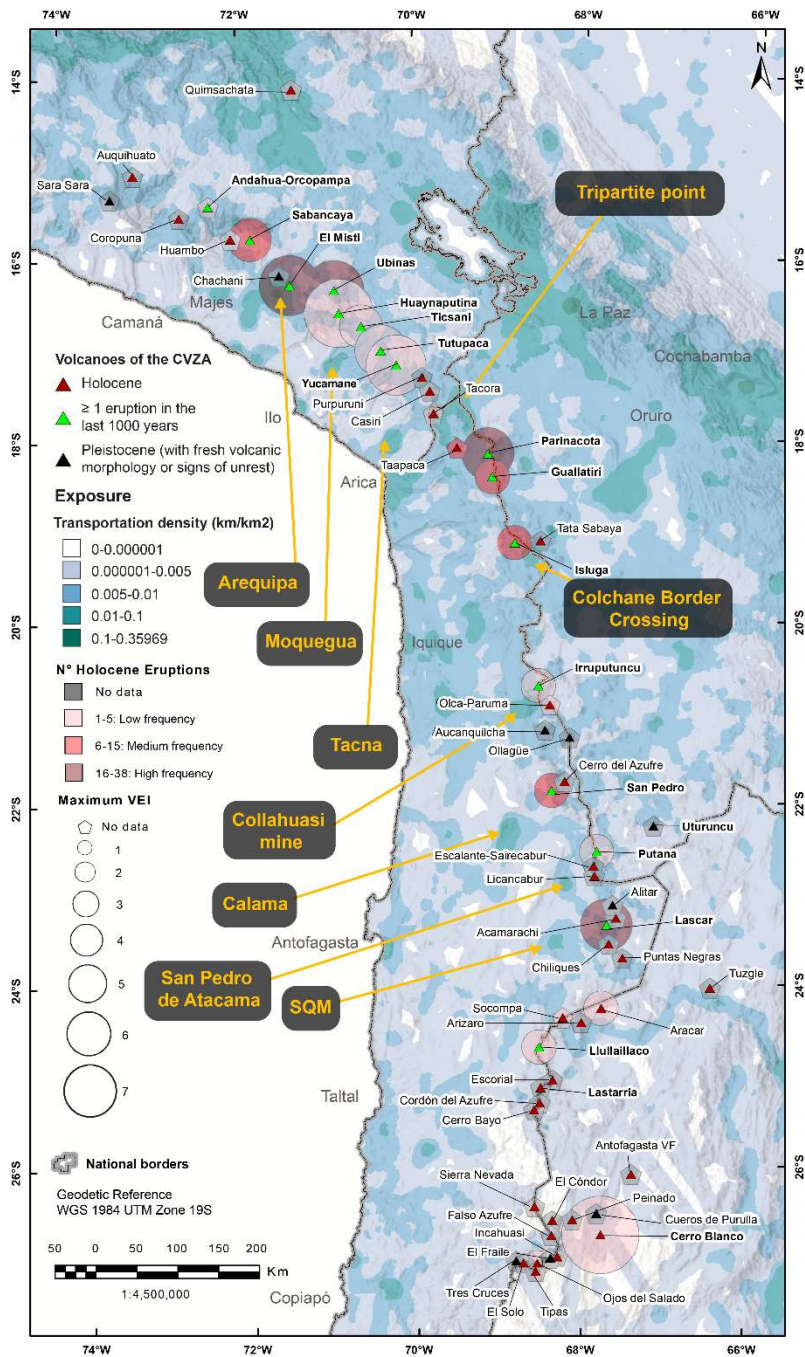
305

Figure 3: Regional map including the total CVZA active and potentially active volcanoes and transportation density, with the Maximum VEI during the Holocene and the number of Holocene eruptions of the CVZA volcanoes superimposed. Notice that the 19 volcanoes considered for the VRR analysis are in bold. Layer Sources: Esri, USGS, NOAA.

Figure 4: Regional map including the total CVZA active and potentially active volcanoes and facilities density, with the Maximum VEI during the Holocene and the number of Holocene eruptions of the CVZA volcanoes superimposed. Notice that the 19 volcanoes considered for the VRR analysis are in bold. Layer Sources: Esri, USGS, NOAA.

15

4.2 The Volcanic Risk Ranking

The 19 out of the 59 CVZA active and potentially active volcanoes that had an eruption during the last 1,000 years or have significant records of unrest signals were ranked based on the four normalized factors of the VRR, i.e., hazard, exposure, vulnerability and resilience (Fig. 5). It is important to first analyse the risk factors separately to better understand what they represent and how they contribute to the overall VRR (Fig. 6). The top five volcanoes showing the highest hazard score are Ubinas (Peru), Lascar (Chile), Sabancaya (Peru), Yucamane (Peru), and Huaynaputina (Peru) (Fig. 5a). The top five volcanoes with the highest exposure score are El Misti (Peru), Ticsani (Peru), Yucamane (Peru), Ubinas (Peru), and Andahua-Orcopampa (Peru) (Fig. 5b). The volcanoes associated with the highest vulnerability scores are Andahua-Orcopampa (Peru), Guallatiri (Chile), Tutupaca (Peru), Ticsani (Peru) and Lastarria (Chile-Argentina) (Fig. 5c). Finally, the top five volcanoes with the highest resilience scores are El Misti (Peru), Ubinas (Peru), Lascar (Chile), Sabancaya (Peru) and Isluga (Chile) (Fig. 5d).
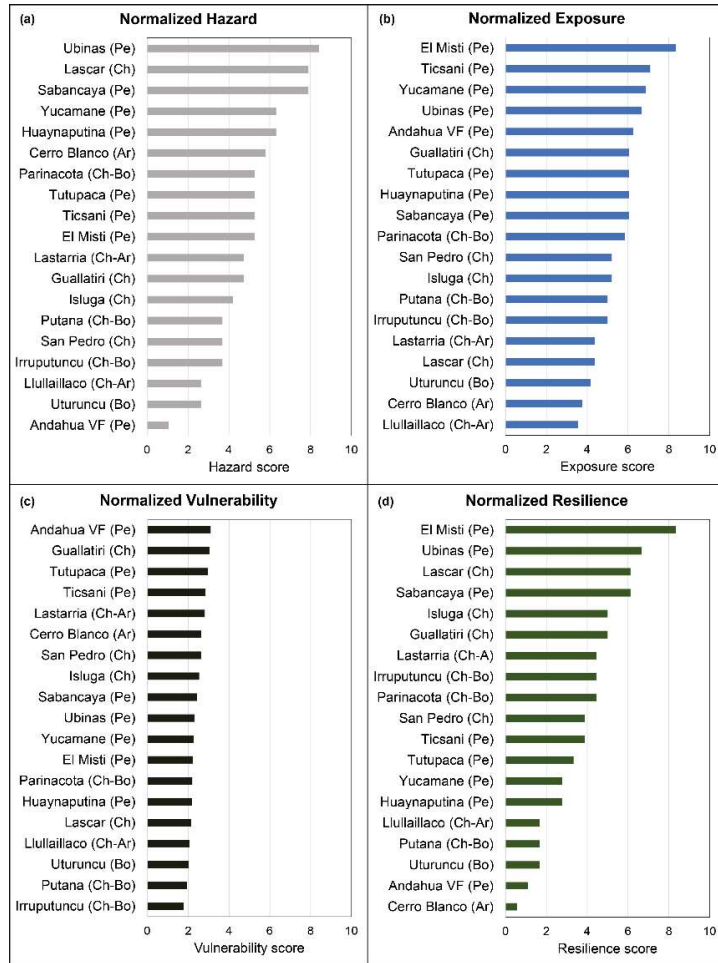
Figure 5: Factors of the volcanic risk ranking analysed separately. (a) hazard scoring; (b) exposure scoring; (c) vulnerability scoring; and (d) resilience scoring.

16

When VRR factors are combined, the top five volcanoes with the highest VRR-0 scores (i.e., hazard and exposure) are Ubinas, Sabancaya, El Misti, Yucamane, and Huaynaputina (Peru) (Fig. 6a); the volcanoes with the five highest VRR-1 scores (i.e., hazard, exposure, vulnerability) are Ubinas, Sabancaya, Ticsani, Yucamane, and El Misti (Peru) (Fig. 6b); while the top five
330 volcanoes with the highest VRR-2 scores (i.e., hazard, exposure, vulnerability and resilience) are Cerro Blanco (Argentina), Yucamane, Huaynaputina, Tutupaca, and Ticsani (Peru) (Fig. 6c).
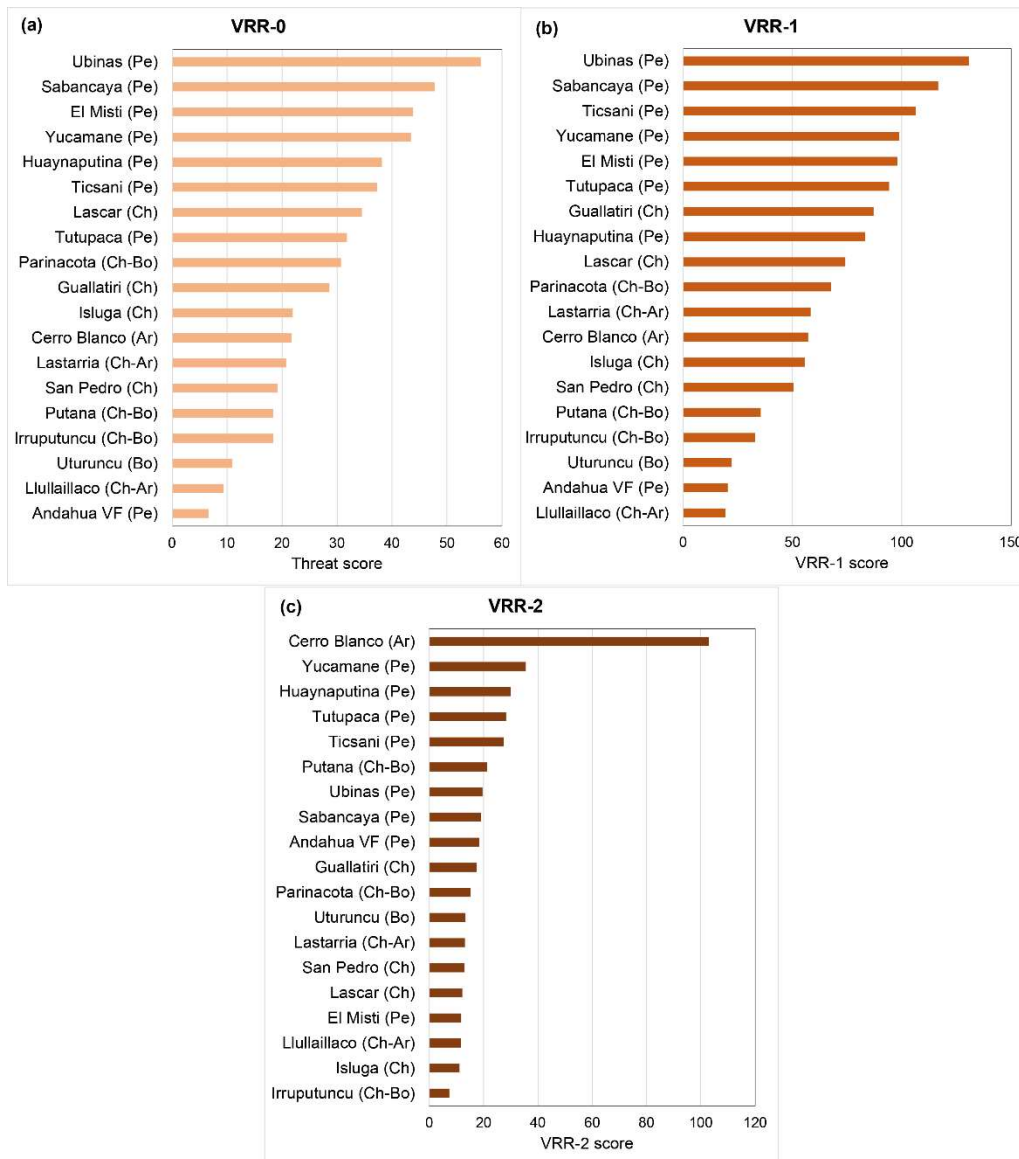
Figure 6: (a) The 2-factor (VRR-0), (b) 3-factor (VRR-1), and (c) 4-factor volcanic risk ranking (VRR-2) applied to the 19 CVZA
335 **selected volcanoes.**

17

5 Discussion

5.1 Significance of regional mapping and VRR for the CVZA

Regional maps allow for a spatial representation of the areas with a high potential for volcanic impact based on the identification of volcanoes with the largest eruptions and the highest eruptive frequency, as well as the highest density of elements at risk (e.g., population, transport infrastructure, emergency and critical facilities) (Figs. 2-4). As an example, the transport-density map highlights the areas having a high concentration of rural and urban infrastructure, which could be potentially impacted with economic consequences for the country. This is the case of the Collahuasi mining district in Chile (https://www.collahuasi.cl/en/quienes-somos/nuestra-historia/). Nonetheless, these regional maps do not provide the details at local scale (e.g., the type or quality of transport infrastructure and facilities). Our regional maps of the CVZA provide a first preliminary step to quickly identify target areas that require a more detailed risk analysis, making them useful for stakeholders. The VRR methodology, on the other hand, provides a more spatially discretized and in-depth relative risk analysis that considers 9 hazard, 9 exposure, 10 vulnerability and 13 resilience parameters (Nieto-Torres et al., 2021 and Guimarães et al., 2021). The analysed elements at risk include population, residential buildings and critical infrastructures exposed within four distance radii (i.e., 5, 10, 30 and 100 km), which cover the areas most susceptible to the impact of the different types of hazards such as tephra fallout, pyroclastic density currents and lahars. In the case of volcanic fields and calderas, the exposure is analysed for elements inside the volcanic field and for the same radii starting from the field's boundary which is defined by the contour connecting the outermost volcanic edifices. Differences in the hierarchy of the volcanoes evaluated within the results of the VRR-0, VRR-1 and VRR-2 are mostly due to population density and the diversity of critical infrastructures considered with the more densely populated areas obtaining higher scores in the threat ranking (i.e., VRR-0). The vulnerability factor in VRR-1 differentiates volcanic systems with equal or similar threat highlighting those associated with larger vulnerabilities (e.g., due to low redundancy and accessibility), while the resilience factor in VRR-2 helps to identify volcanoes with no or few mitigation and response measures. The variability between the results of the various VRR approaches (e.g., equations 1–3) confirm the importance of including hazard, exposure, vulnerability and resilience in an integrative ranking analysis to capture the risk complexity and best prioritize risk reduction strategies (Fig. 5, 6). Broad common patterns between the regional maps and the VRR are discussed below.

From a hazard perspective, both the regional maps (Fig. 2-4) and the hazard factor of the VRR (Fig. 5a) allow to identify Ubinas (Peru), Lascar (Chile), Huaynaputina (Peru) and Cerro Blanco (Argentina) as the most hazardous volcanoes. Although El Misti (Peru) and Parinacota (Chile) have a high eruptive frequency (22 and 38 events during the Holocene), they occupy only the 10th and 7th position on the hazard factor of the VRR, respectively. The reason is that overall, the maximum hazard score on the VRR represents the highest intensity of each volcanic process, not only eruptive frequency and maximum VEI as in the regional mapping. On the contrary, Sabancaya and Yucamane (Peru) appear at the 3rd and 4th position on the normalized

18

hazard factor of the VRR but are not highlighted in the regional maps since they have a medium to low eruptive frequencies (14 and 1 event, respectively); and maximum VEIs (3 and 5, respectively).

370

It is worth noticing that the basis of focusing in the last 1,000 years of volcanic activity for the VRR analysis is in line with the methodology proposed by Nieto-Torres et al. (2021) and applied by Guimaraes et al. (2021). Nieto-Torres et al. (2021) found that the volcanoes associated with the highest risk score for Mexican volcanoes were the same, regardless of the analysed time window of eruption occurrence (i.e., <1 and <10 ka). Additionally, Guimaraes et al. (2021), who first applied this

375 methodology on Latin American volcanoes, found that this criterion considers the better constrained eruptions in the eruptive records. The grouping of volcanoes based on the age, most recent eruptions and eruption periodicities has also been previously used to rank volcanoes in a general order of "decreasing concern" (e.g., Bailey et al., 1983) and currently the occurrence of eruptions within the last 1,000 years represents one of the controlling factors in developing strategies to increase resilience (Nieto-Torres et al., 2021). However, focusing only on volcanoes with eruptions in the last 1,000 years might exclude

380 potentially impactful volcanoes. For this reason, we also considered for the VRR analysis three additional volcanoes that show three signs of unrest: Uturuncu, Lastarria, and Cerro Blanco. For a more comprehensive analysis and to confirm our preliminary results, future works could apply the VRR to all 59 active and potentially active volcanoes.

When hazard and exposure are considered, both regional mapping and VRR-0 highlight Ubinas, El Misti, and Huaynaputina as the volcanoes with the highest potential risk (Figs. 2-4 and 6a). However, Sabancaya and Yucamane appear on the 2nd and

385 4th positions of the threat score (VRR-0) but are not highlighted on the regional mapping. The reason is that the regional map only considers the number of Holocene eruptions and maximum VEI as hazard parameters, with an overlap on the different layers of elements at risk, whilst the VRR evaluates the interaction of 9 hazard and 9 exposure parameters at different radii from the volcanic vent, making it a more exhaustive analysis.

390

The vulnerability factor, which is not considered for the regional mapping, helps to best distinguish volcanic systems with similar threat (i.e., VRR-0, H×E) but different vulnerabilities (e.g., Irruputuncu and Putana volcanoes, Chile). In particular, the variety of parameters related to the systemic vulnerability helps to highlight the volcanoes with high exposure and low redundancy and accessibility to infrastructures (e.g., Ticsani volcano, Peru). Finally, the inclusion of resilience in VRR-2

395 contributes to highlight those systems with moderate (e.g., Tutupaca, Huaynaputina, Peru; and Cerro Blanco, Argentina) to high score (e.g., Ticsani and Yucamane, Peru) in the VRR-1 (Fig. 6b) but having none or few resilience measures implemented (Fig. 5d) (Guimarães et al., 2021). In fact, whilst the inclusion of vulnerability only affects a few volcanoes (VRR-0 versus VRR-1, Fig. 6a-b), the influence of resilience is quite remarkable for all volcanoes, highlighting those systems with none or few mitigation and response (resilience) measures implemented (i.e., Cerro Blanco, Argentina; Yucamane, Huaynaputina,

400 Tutupaca, and Ticsani, Peru) (Fig. 6c). As an example, Ubinas (Peru) has the highest normalized score in terms of hazard and medium normalized score in terms of vulnerability, but the second highest normalized score in terms of resilience (see Fig. 5),

19

which explains the 1st position in the VRR-1 and the 7th position in the VRR-2 (Fig. 6b-c). The systems taking the top positions of the VRR-2 are those either with high hazard, medium-high exposure, and vulnerability scores, or those with few to no mitigation and response measures implemented (e.g., Cerro Blanco, Argentina; Yucamane, Huaynaputina, Tutupaca, and Ticsani, Peru). Cerro Blanco (Argentina) scores as the highest risk volcano of the CVZA due to its low resilience (Fig. 6c).

Overall, as different dimensions of vulnerability are closely related to the elements at risk, it is important to rethink land-use planning to not increase or create new risk. To reduce vulnerability, it is advisable to create redundancy (e.g., alternative power infrastructure within 100 km of Cerro Blanco) and accessibility to critical infrastructure (e.g., connections to power, water, telecommunication and emergency facilities within 100 km of Cerro Blanco, Ticsani and Tutupaca volcanoes). In addition, diversification of economic activities should be promoted, especially within 5-30 km around Cerro Blanco, Tutupaca, Ticsani, Ubinas and Sabancaya volcanoes. Priority risk reduction strategies that should be put in place or improved in order to increase resilience are listed below. First, volcanic records should be better constrained at target volcanoes in order to compile up-to-date hazard assessments. Within the top five VRR-1 and VRR-2 high risk volcanoes, only Cerro Blanco has no hazard maps, but it is important to make sure that the existent ones are up-to-date and available for the entire community. Second, the monitoring systems should be improved for Tutupaca (basic real time), Huaynaputina and Yucamane (limited) and implemented at Cerro Blanco (non-existent). Third, efforts should be made to compile risk assessments; this is missing at all these five highest-risk volcanoes (Cerro Blanco, Yucamane, Huaynaputina, Tutupaca, and Ticsani). Fourth, educational activities should be promoted to raise awareness in populations living around Ticsani, Yucamane, Huaynaputina, Tutupaca, and Cerro Blanco; and existing ones should be supported and strengthened around Ubinas, Sabancaya and El Misti. Finally, local authorities could invest in preparedness (e.g., evacuation plans and exercises or simulations for institutions and the population), insurance coverage, engineering mitigation measures and implementation of early warning systems.

5.2 Comparison with existing volcanic rankings

To visualize the different existing volcanic rankings, we have collected the threat and risk scores in a comparative diagram shown in Fig. 7. At the time of our investigation, three of the four CVZA countries have already developed a relative volcanic threat ranking (i.e., Peru, Chile and Argentina) based on the methodology proposed by Ewert et al. (1998; 2005), in addition to the study of Guimarães et al. (2021) applying the VRR strategy to Latin American volcanoes with activity recorded in the last 1,000 years. The comparison between these rankings is not straightforward because they consider the risk factors in different ways. Consequently, we can find relative threat and risk scores ranging from 0 to 250 (Fig. 7). In addition, each country evaluates only the volcanoes that concern their own territory whilst our VRR strategy considers volcanoes from the four CVZA countries. Regardless of the relative scoring, this difference of approaches is evidenced in Fig. 7 by the clustering of volcanoes per country.

20
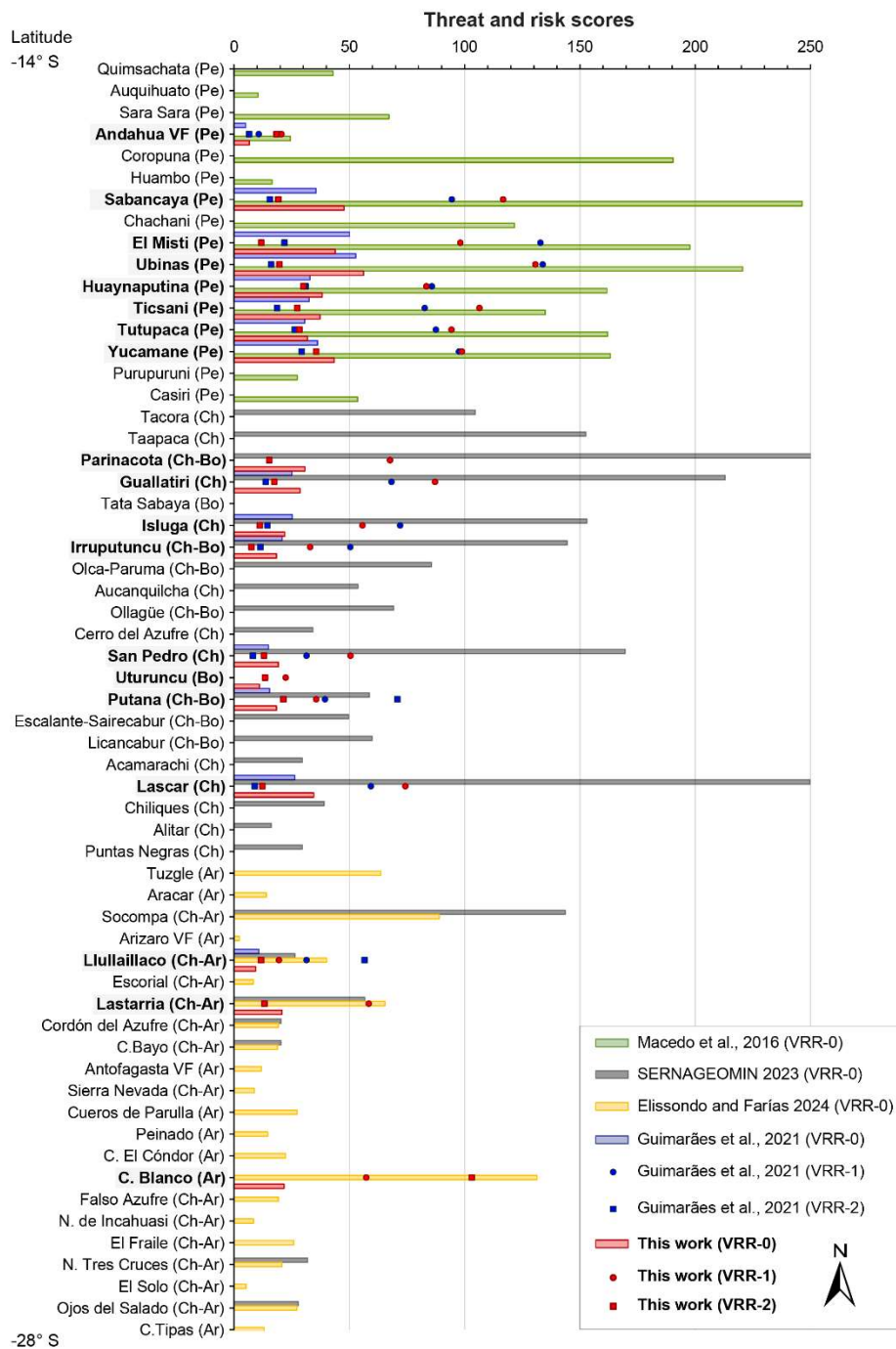
Figure 7: Comparison of existing volcanic threat and risk rankings. The CVZA volcanoes are organized by latitude, the volcanic systems in bold highlight the 19 analysed for the VRR in this work. Notice that bars represent threat rankings (i.e., VRR-0 (HxE)), circles represent the 3-factor VRR-1, and squares the 4-factor VRR-2. The threat ranking of INGEMMET (Macedo et al., 2016) in green, SERNAGEOMIN (SERNAGEOMIN, 2023) in grey, SEGEMAR (Elissondo and Farías, 2024) in yellow, the threat and risk rankings of Guimarães et al. (2021) in blue, and the ones of this work in red.

21

Comparing threat rankings in particular, we can point out that three of the five rankings share the same volcanoes in the top five, with slight differences in the order (Table 3, Fig. 7). The difference for the VRR-0 between this study and Guimarães et

440 al. (2021) is related to the update of data used, and subsequently the scoring of some indicators such as the recurrence rate. The difference with Macedo et al. (2016) is the absence of Coropuna volcano (Peru) in the list. Interestingly, Coropuna has a higher exposure than Huaynaputina, but was not considered in the work of Guimarães et al. (2021) nor in this study because it does not have records of eruptions during the last 1,000 years, nor the three signs of unrest. The Chilean and Argentinian threat rankings are not directly comparable since their rankings do not consider volcanoes outside their territory and there is

445 no existing ranking for Bolivian volcanoes.

Table 3. Comparison of the top 5 CVZA volcanoes of existing threat rankings considering hazard and exposure (VRR-0). Pe: Peru, Ch: Chile, Bo: Bolivia, Ar: Argentina. Underlined volcanoes highlight the ones appearing in different threat rankings.

	This work VRR-0	Guimarães et al. (2021) VRR-0	SERNAGEOMIN (2023)	Elissondo and Farias (2024)	Macedo et al. (2016)
1	Ubinas (Pe)	Ubinas (Pe)	Lascar (Ch)	Cerro Blanco (Ar)	Sabancaya (Pe)
2	Sabancaya (Pe)	El Misti (Pe)	Parinacota (Ch-Bo)	Socompa (Ch-Ar)	Ubinas (Pe)
3	El Misti (Pe)	Yucamane (Pe)	Guallatiri (Ch)	Lastarria (Ch-Ar)	El Misti (Pe)
4	Yucamane (Pe)	Sabancaya (Pe)	San Pedro (Ch)	Tuzgle (Ar)	Coropuna (Pe)
5	Huaynaputina (Pe)	Huaynaputina (Pe)	Isluga (Ch)	Llullaillaco (Ch-Ar)	Yucamane (Pe)

450 When comparing the existing threat rankings without the Peruvian volcanoes (Table 4), it is interesting to notice that the top-ranked volcano is the same for Guimarães et al. (2021), SENARGEOMIN, (2023) and this work, i.e., Lascar volcano located in Chile. With respect to the Chilean or transboundary volcanoes, the top three volcanoes are the same between our ranking and the one of SERNAGEOMIN. Then, the Cerro Blanco volcano, which is the top-ranked Argentinian CVZA volcano, appears fifth in our threat ranking. It was considered in our work due to the fact that it has shown the three signs of unrest.

455 Except for this volcano, none of the volcanoes listed by Elissondo and Farias (2024) appears in the top five in the other rankings. This demonstrates the influence of the scale of analysis, country versus region.

Table 4. Comparison of the top 5 CVZA volcanoes of existing threat rankings, considering hazard and exposure (VRR-0) only for Chilean and Argentinian volcanoes. Ch: Chile, Bo: Bolivia, Ar: Argentina. Underlined volcanoes highlight the ones appearing in
460 **different threat rankings.**

	This work VRR-0	Guimarães et al. (2021) VRR-0	SERNAGEOMIN (2023)	Elissondo and Farias (2024)
1	Lascar (Ch)	Lascar (Ch)	Lascar (Ch)	Cerro Blanco (Ar)
2	Parinacota (Ch-Bo)	Isluga (Ch)	Parinacota (Ch-Bo)	Socompa (Ch-Ar)
3	Guallatiri (Ch)	Guallatiri (Ch)	Guallatiri (Ch)	Lastarria (Ch-Ar)
4	Isluga (Ch)	Irruputuncu (Ch-Bo)	San Pedro (Ch)	Tuzgle (Ar)
5	Cerro Blanco (Ar)	Putana (Ch-Bo)	Isluga (Ch)	Llullaillaco (Ch-Ar)

When accounting for the vulnerability and resilience factors (VRR-1 and VRR-2), only this work and that of Guimarães et al. (2021) can be compared (Table 5, Fig. 7). When hazard, exposure and vulnerability are combined, both approaches highlight Ubinas, Sabancaya, El Misti and Yucamane within the top five VRR-1 volcanoes. However, Ticsani appears in the 3rd position

22

of our ranking and in the 7th position of Guimarães et al. (2021), whilst Tutupaca is in the 5th in Guimarães et al. (2021) and the 6th position in our ranking. Both volcanoes have the same hazard scores in both studies, however, Ticsani has a higher exposure score in our work, and hence, although its vulnerability is lower than Tutupaca, it scores higher in the VRR-1 produced in this work. The reasons for this are i) a higher population density identified within the 10, 30 and 100 km radii in our work; ii) telecommunications score, not considered in Guimarães et al. (2021); and iii) the multiple economic activity source within 100 km for both volcanoes that have been updated with respect to Guimarães et al. (2021).

Table 5. Comparison of the top 5 CVZA volcanoes of existing risk rankings, considering hazard, exposure, vulnerability VRR-1 and resilience VRR-2. Pe: Peru, Ch: Chile, Bo: Bolivia, Ar: Argentina. Underlined volcanoes highlight the ones repeated in both ranking stategies.

	This work VRR-1	Guimarães et al. (2021) VRR-1	This work VRR-2	Guimarães et al. (2021) VRR-2
1	Ubinas (Pe)	Ubinas (Pe)	Cerro Blanco (Ar)	Putana (Ch-Bo)
2	Sabancaya (Pe)	El Misti (Pe)	Yucamane (Pe)	Llullaillaco (Ch-Ar)
3	Ticsani (Pe)	Yucamane (Pe)	Huaynaputina (Pe)	Huaynaputina (Pe)
4	Yucamane (Pe)	Sabancaya (Pe)	Tutupaca (Pe)	Yucamane (Pe)
5	El Misti (Pe)	Tutupaca (Pe)	Ticsani (Pe)	Tutupaca (Pe)

Larger differences are found when considering resilience (VRR-2 in Table 5 and Fig. 7). Both studies share three volcanoes in the top five, Yucamane, Huaynaputina and Tutupaca, although in different orders. However, Cerro Blanco and Ticsani appear in the 1st and 5th position of our VRR-2, respectively, whilst Putana and Llullaillaco are in the 1st and 2nd position of Guimarães et al., (2021) but only in the 6th and 17th positions of our VRR-2. There are significant differences in several parameters used in scoring these volcanoes in both studies due to a better knowledge of the CVZA volcanoes as well as the available vulnerability and resilience data. Few examples are discussed below.

With a VEI of 7, Cerro Blanco represents an important case for the CVZA since its last caldera eruption is one of the largest Holocene eruptions worldwide (Fernandez-Turiel et al., 2019). Whilst it was not considered by Guimarães et al. (2021), because it has not erupted in the past 1,000 years, we account for the presence of unrest signs, in agreement with SERNAGEOMIN criteria. From the regional map analysis, we also found that there are important localities within 100 km radius around Cerro Blanco, such as Antofagasta de la Sierra or Corral Quemado (with 730 and 1200 inhabitants, respectively).

In the case of Putana, it has the same hazard score, but higher exposure, lower vulnerability and higher resilience scores leading to a lower overall VRR-2 in this work with respect to Guimarães et al. (2021). Regarding Lullaillaco volcano, it has a lower hazard and vulnerability scores and higher exposure and resilience scores, leading to a lower overall VRR-2 in our work in contrast to Guimarães et al. (2021). The largest differences for these two volcanoes are found in the vulnerability scoring given by the typology of buildings, its proximity to the Argentina-Chile border, the lack of redundancy of power and telecommunication infrastructures and the multiple economic activities within 30 km radius. In addition, according to our

495 updated information, there are existing hazard maps for Putana volcano (Amigo et al., 2012) increasing its resilience score with respect to Guimarães et al. (2021).

5.3 Data limitations

It is important to notice the dynamic dimension of all risk factors and emphasize that the parameters of the rankings can be easily updated when new information becomes available, consequently modifying the final score (e.g., Guimarães et al., 2021
500 versus this work). This is particularly true for the CVZA given the large uncertainties associated with this volcanic zone. Factor scoring highly depends on the availability, quality and accuracy of data, for both regional mapping and VRR analysis. The complexity and diversity of volcanic hazards and their impacts can exacerbate existing cross-border differences with respect to hazard information, elements at risk, vulnerability, scientific resources, disaster management, mitigation capacity, and public awareness. These differences affect the development of research, sharing of data, accessibility to the information, expertise
505 and resources, and, consequently, the availability and analysis of data (Donovan and Oppenheimer, 2019). Therefore, one of the main challenges for this study was the accessibility to the same level of precision and heterogeneity of available datasets across countries, in terms of format, taxonomy (e.g., different names for building types or roads), spatial and temporal resolutions. As previous works (e.g., Guimarães et al., 2021), we also recognize the limitations of the Global Volcanism Program database especially in relation to the eruptive history. For example, after the last update, San Pedro volcano is now
510 listed as Pleistocene (GVP, 2023b), being catalogued previously as Holocene (GVP, 2013), with 10 eruptive events and maximum VEI 2, also in agreement with SERNAGEOMIN. In the case of Parinacota volcano, the number of eruptions is also not consistent, i.e., six according to the GVP (2023), and at least 38 after the updated hazard map recently published by SERNAGEOMIN (Bertin et al., 2022b). Another case is Yucamane volcano, for which the GVP (2023) lists its last eruption as 1320 BCE, which would leave this volcano out of our VRR analysis but according to INGEMMET its last eruption was
515 1787 CE (Macedo et al., 2016). Additionally, the timeliness of data, in particular for the elements at risk and their vulnerability, is highly variable, influencing the accuracy of the analysis.

6 Conclusions

Regional mapping and volcanic risk rankings represent important tools to identify volcanoes requiring a prioritization of strategies and efforts in volcanic risk reduction. However, the final results strongly depend on the assumptions of the selected
520 VRR methodology and on the availability of data. The selection of volcanoes to evaluate can also vary depending on the objective of the study. Our analysis shows that the most comprehensive list of volcanoes of the CVZA currently comprises a total of 59 active and potentially active volcanic centres. However, this number could change in the future if additional information on the various volcanoes becomes available.

525 The regional maps compiled for a general visualization of hazard and elements at risk for the 59 volcanoes show that:

24

- Huaynaputina and Cerro Blanco are the volcanoes with the highest eruption magnitude (VEI 6 and VEI 7, respectively) and the volcanoes with the highest eruption frequency are El Misti (22), Ubinas (26), Parinacota (38) and Lascar (37).

530
- Arequipa, Moquegua, and Tacna (Peru), Calama and the mining stations "Estación Zaldivar" and "Mina Escondida" (Chile) are associated with the highest population density per km^2.

- Arequipa, Moquegua, and Tacna cities (Peru), the tripartite point and Colchane customs post (between Peru-Bolivia-Chile and Bolivia-Chile, respectively), and the Collahuasi mining district, Calama city, San Pedro de Atacama town, and Sociedad Química y Minera de Chile (Chile) are associated with the highest density of transport infrastructure per km^2.

535
- Arequipa (Peru) is associated with the highest density of facilities per km^2.

The most threatening volcanoes according to our regional mapping are El Misti and Ubinas, as they are the closest to Arequipa city (Peru), which represents the most densely populated area, also associated with the highest density of transport infrastructure and facilities per km^2.

540 While the regional maps provide a visual assessment of potential volcanic impact at a regional scale, the VRR provides a more comprehensive regional analysis by integrating four different risk factors. In this study, the VRR was focused on the 19 active or potentially active volcanoes that erupted in the last 1,000 years and/or show significant signs of unrest. Results allow to identify the highest risk volcanoes and those that need to be prioritized in terms of implementing risk reduction strategies. In particular:

545
- The VRR-0, which considers hazard and exposure, highlights Ubinas, Sabancaya, El Misti, Yucamane and Huaynaputina as the most threatening volcanoes.

- The VRR-1, which considers hazard, exposure, and vulnerability, highlights Ubinas, Sabancaya, Ticsani, Yucamane, and El Misti as the highest-risk volcanoes,

- The VRR-2, which also includes resilience parameters, identifies Cerro Blanco, Yucamane, Huaynaputina, Tutupaca,
550 and Ticsani as the highest-risk volcanoes.

- Given that volcanic hazard and exposure are difficult to modify and reduce, the implementation of risk reduction strategies should focus on reducing vulnerability and increasing resilience, which are highlighted by the results of VRR-1 and VRR-2.

We encourage the use of volcanic risk rankings to characterize volcanic systems and support risk reduction strategies at a
555 regional scale, which is especially valuable in the case of cross-border volcanoes. In fact, risk rankings are often carried out at a national level, neglecting the complexity of crisis management in case of cross-border eruptions. In the case of the CVZA, most volcanoes are located within less than 25 km from an international border and at least 20 of them share borders, which

could result in challenging crisis managements and complex impact patterns. With the hope that our work promotes cooperation between CVZA countries to increase resilience through the co-production of hazard and risk maps, the

560 development of coordinated emergency plans and co-creation of protocols to manage potential impacts, we recommend to carry out further studies at different scales, and to continuously update the presented regional VRR as new information becomes available.

7 Competing interests

The authors declare that they have no conflict of interest.

565 **8 Author Contributions**

MPRH carried out the compilation of hazard and resilience parameters with the contribution of ME, SG, RA, and GP. LSDM carried out the compilation of exposure and vulnerability parameters with the contribution of LD and CF. MPRH, LSDM and LF carried out the Volcanic Risk Ranking. MPRH and LSDM carried out the regional mapping and drafted the first draft of the manuscript with the contribution of LD, CF, SB, and CB. All authors contributed to the finalization of the manuscript.

570 **9 Funding**

10 Acknowledgements

580 **References**

Aguilar, R., Thouret, J.-C., Samaniego, P., Wörner, G., Jicha, B., Paquette, J.-L., Suaña, E., and Finizola, A.: Growth and evolution of long-lived, large volcanic clusters in the Central Andes: The Chachani Volcano Cluster, southern Peru, J.

26

Volcanol. Geotherm. Res., 426, 107539, https://doi.org/10.1016/j.jvolgeores.2022.107539, 2022.

Aguilera, F.: Origen y naturaleza de los fluidos en los sistemas volcánicos, geotermales y termales de baja entalpía de la Zona
585   Volcánica Central entre los 17°43´S y 25°10´S, Chile, Ph.D. Thesis. Univ. Católica del Norte. (In Spanish), 393, 2008.

Aguilera, F., Viramonte, J., Medina, E., Guzmán, K., Becchio, R., Delgado, H., and Arnosio, M.: Eruptive Activity From
Lascar Volcano (2003 – 2005), XI Congr. Geológico Chil. Antofagasta, II Región, Chile, 2, 397–400, 2006.

Aguilera, F., Tassi, F., Darrah, T., Moune, S., and Vaselli, O.: Geochemical model of a magmatic–hydrothermal system at the
Lastarria volcano, northern Chile, Bull. Volcanol., 74, 119–134, https://doi.org/10.1007/s00445-011-0489-5, 2012.

590   Aguilera, F., Layana, S., Rodríguez-Díaz, A., González, C., Cortés, J., and Inostroza, M.: Hydrothermal alteration, fumarolic
deposits and fluids from Lastarria Volcanic Complex: A multidisciplinary study, Andean Geol., 43, 166,
https://doi.org/10.5027/andgeoV43n2-a02, 2016.

Aguilera, F., Layana, S., Rojas, F., Arratia, P., Wilkes, T. C., González, C., Inostroza, M., McGonigle, A. J. S., Pering, T. D.,
and Ureta, G.: First measurements of gas flux with a low-cost smartphone sensor-based uv camera on the volcanoes of Northern
595   Chile, Remote Sens., 12, https://doi.org/10.3390/rs12132122, 2020.

Aguilera, F., Apaza, F., Del Carpio, J., Grosse, P., Jiménez, N., Ureta, G., Inostroza, M., Báez, W., Layana, S., Gonzalez, C.,
Rivera, M., Ortega, M., Gonzalez, R., and Iriarte, R.: Advances in scientific understanding of the Central Volcanic Zone of
the Andes: a review of contributing factors, Bull. Volcanol., 84, 1–8, https://doi.org/10.1007/s00445-022-01526-y, 2022.

Amigo, A., Bertin, D., and Orozco, G.: Peligros volcanicos de la zona norte de Chile, Regiones de Arica y Parinacota, Tarapacá,
600   Antofagasta y Atacama. Servicio Nacional de Geología y Minería, Carta Geológica de Chile, Serie Geología Ambiental, 2012.

Anderssohn, J., Motagh, M., Walter, T. R., Rosenau, M., Kaufmann, H., and Oncken, O.: Surface deformation time series and
source modeling for a volcanic complex system based on satellite wide swath and image mode interferometry: The Lazufre
system, central Andes, Remote Sens. Environ., 113, 2062–2075, https://doi.org/10.1016/j.rse.2009.05.004, 2009.

Antayhua, Y., Ramos, D., and Masías, P.: Monitoreo de los volcanes Ticsani, Sabancaya y Huaynaputina: Periodo 2006-2012,
605   INGEMMET, Boletín No 53 Ser. C Geodinámica e Ing. Geológica, 124, 2013.

Apaza, F., Kern, C., Ortega, M., and Miranda, R.: The July 2019 explosive activity of Ubinas Volcano , Peru, EGU21-3529,
1, https://doi.org/https://doi.org/10.5194/egusphere-egu21-3529, 2021.

Auker, M. R., Sparks, R. S. J., Jenkins, S. F., Aspinall, W., Brown, S. K., Deligne, N. I., Jolly, G., Loughlin, S. C., Marzocchi,
W., Newhall, C. G., and Palma, J. L.: Development of a new global Volcanic Hazard Index (VHI), in: Global Volcanic Hazards
610   and Risk, Cambridge University Press, 349–358, https://doi.org/10.1017/CBO9781316276273.024, 2015.

Báez, W., Arnosio, M., Chiodi, A., Ortiz-Yañes, A., Viramonte, J. G., Bustos, E., Giordano, G., and López, J. F.: Stratigraphy
and evolution of the Cerro Blanco Volcanic Complex, Puna Austral, Argentina, Rev. Mex. Ciencias Geológicas, 32, 29–49,
2015.

Bailey, R. A., Beauchemin, P. R., Kapinos, F. P., and Klick, D. W.: The Volcano Hazards Program: objectives and long-range
615   plans, Open-File Rep. 83-400. Reston, VA U.S. Geol. Surv., 33 p, https://doi.org/10.3133/ofr83400, 1983.

Barazangi, M. and Isacks, B. L.: Spatial distribution of earthquakes and subduction of the Nazca plate beneath South America,

27

Geology, 4, 686, https://doi.org/10.1130/0091-7613(1976)4<686:SDOEAS>2.0.CO;2, 1976.

Barberi, F., Coltelli, M., Ferrara, G., Innocenti, F., Navarro, J. M., and Santacroce, R.: Plio-Quaternary volcanism in Ecuador, Geol. Mag., 125, 1–14, https://doi.org/10.1017/S0016756800009328, 1988.

620 Bertin, D.: Volcano-tectonic history and volcanic hazard assessment of the 22.5-29 °S segment of the Central Volcanic Zone of the Andes, Dr. Diss. Res. Space@ Auckland. Univ. Auckl., 248, 2022.

Bertin, D., Lindsay, J. M., Cronin, S. J., de Silva, S. L., Connor, C. B., Caffe, P. J., Grosse, P., Báez, W., Bustos, E., and Constantinescu, R.: Probabilistic Volcanic Hazard Assessment of the 22.5–28°S Segment of the Central Volcanic Zone of the Andes, Front. Earth Sci., 10, https://doi.org/10.3389/feart.2022.875439, 2022a.

625 Bertin, L. ., Jara, G. ., and Toloza, V.: Peligros del volcán Parinacota, región de Arica y Parinacota. Servicio Nacional de Geología y Minería, Carta Geológica de Chile, Serie de Geología Ambiental: X p., 1 mapa escala 1:50.000, Santiago., 2022b.

BGVN: Report on Sabancaya (Peru) (Crafford, A.E., and Venzke, E., eds.), Glob. Volcanism Program, 2021. Bull. Glob. Volcanism Network. Smithson. Institution., 46, 2021.

Bredemeyer, S., Ulmer, F.-G., Hansteen, T., and Walter, T.: Radar Path Delay Effects in Volcanic Gas Plumes: The Case of
630 Láscar Volcano, Northern Chile, Remote Sens., 10, 1514, https://doi.org/10.3390/rs10101514, 2018.

Bromley, G. R. M., Thouret, J.-C., Schimmelpfennig, I., Mariño, J., Valdivia, D., Rademaker, K., del Pilar Vivanco Lopez, S., Team, A., Aumaître, G., Bourlès, D., and Keddadouche, K.: In situ cosmogenic 3He and 36Cl and radiocarbon dating of volcanic deposits refine the Pleistocene and Holocene eruption chronology of SW Peru, Bull. Volcanol., 81, 64, https://doi.org/10.1007/s00445-019-1325-6, 2019.

635 Brunori, C. A., Bignami, C., Stramondo, S., and Bustos, E.: 20 years of active deformation on volcano caldera: Joint analysis of InSAR and AInSAR techniques, Int. J. Appl. Earth Obs. Geoinf., 23, 279–287, https://doi.org/10.1016/j.jag.2012.10.003, 2013.

Budach, I., Brasse, H., and Díaz, D.: Imaging of conductivity anomalies at Lazufre volcanic complex , Northern Chile , through 3-D inversion of magnetotelluric data, Schmucker-Weidelt-Kolloquium Neustadt an der Weinstraße, 27–34, 2011.

640 Byrdina, S., Ramos, D., Vandemeulebrouck, J., Masias, P., Revil, A., Finizola, A., Gonzales Zuñiga, K., Cruz, V., Antayhua, Y., and Macedo, O.: Influence of the regional topography on the remote emplacement of hydrothermal systems with examples of Ticsani and Ubinas volcanoes, Southern Peru, Earth Planet. Sci. Lett., 365, 152–164, https://doi.org/10.1016/j.epsl.2013.01.018, 2013.

Cahill, T. and Isacks, B. L.: Seismicity and shape of the subducted Nazca Plate, J. Geophys. Res., 97, 17503,
645 https://doi.org/10.1029/92JB00493, 1992.

Capaccioni, B., Aguilera, F., Tassi, F., Darrah, T., Poreda, R. J., and Vaselli, O.: Geochemical and isotopic evidences of magmatic inputs in the hydrothermal reservoir feeding the fumarolic discharges of Tacora volcano (northern Chile), J. Volcanol. Geotherm. Res., 208, 77–85, https://doi.org/10.1016/j.jvolgeores.2011.09.015, 2011.

Del Carpio, J. A. and Torres, J. L.: La actividad sísmica en el volcán Ubinas y su variación temporal (1998-2019) para la
650 identificación de patrones de sismicidad a ser considerados en la gestión del riesgo de desastres, 71, 2020.

Centeno, R., Anccasi, R., and Macedo, O.: Sismos distales de fractura observados en la zona de los Volcanes Misti y Chachani, 4, 2013.

Chiodi, A., Tassi, F., Báez, W., Filipovich, R., Bustos, E., Glok Galli, M., Suzaño, N., Ahumada, M. F., Viramonte, J. G., Giordano, G., Pecoraino, G., and Vaselli, O.: Preliminary conceptual model of the Cerro Blanco caldera-hosted geothermal system (Southern Puna, Argentina): Inferences from geochemical investigations, J. South Am. Earth Sci., 94, 102213, https://doi.org/10.1016/j.jsames.2019.102213, 2019.

Clavero, J., Sparks, S., Polanco, E., and Pringle, M.: Evolution of Parinacota volcano, Central Andes, Northern Chile, Rev. geológica Chile, 31, 317–347, https://doi.org/10.4067/S0716-02082004000200009, 2004.

Clavero, J., Soler, V., and Amigo, A.: Caracterización preliminar de la actividad sísmica y de desgasificación pasiva de volcanes activos de los Andes Centrales del Norte de Chile, XI Congr. Geológico Chil. Antofagasta, II Reg. Chile, 2, 443–446, 2006.

Contreras, Á.: Caracterización de la mineralogía de alteración hidrotermal en superficie del Volcán Tacora y sus alrededores, Región de Arica y Parinacota., Mem. para optar al título geólogo, 98, 2013.

Cruz, J.: Análisis de la actividad sísmica en el volcán Ticsani y su variación temporal, periodo 1999-2019, Inf. vulcanológico IGP/CENVUL-TIC/IV 2020-0001, 72, 2020.

Cruz, V., Vargas, V., and Matsuda, K.: Geochemical Characterization of Thermal Waters in the Calientes Geothermal Field, Tacna, South of Peru, Proc. World Geotherm. Congr. 2010, 7, 2010.

Cruz, V., Flores, R., and Velarde, Y.: Caracterización y evaluación del potencial geotérmico de la zona geotermal Casiri-Kallapuma, Región Tacna, NGEMMET, Boletín Ser. B Geol. Económica N° 69, 250, 2020.

Donovan, A. and Oppenheimer, C.: Volcanoes on borders: a scientific and (geo)political challenge, Bull. Volcanol., 81, 31, https://doi.org/10.1007/s00445-019-1291-z, 2019.

Elissondo and Farías: Riesgo volcánico relativo en territorio Argentino., Inst. Geol. y Recur. Miner. Serv. Geológico Min. Argentino. Ser. Contrib. Técnicas Peligrosidad Geológica Nº 28., 99, 2024.

Ewert, J. W., Miller, C. D., Tilling, R. I., and Neal, C. A.: Revised Criteria for Identifying High-Risk Volcanoes Around theWorld., EOS Trans. Am. Geophys. Union., 79, 993, 1998.

Fernandez-Turiel, J. L., Perez–Torrado, F. J., Rodriguez-Gonzalez, A., Saavedra, J., Carracedo, J. C., Rejas, M., Lobo, A., Osterrieth, M., Carrizo, J. I., Esteban, G., Gallardo, J., and Ratto, N.: La gran erupción de hace 4.2 ka cal en Cerro Blanco, Zona Volcánica Central, Andes: nuevos datos sobre los depósitos eruptivos holocenos en la Puna sur y regiones adyacentes, Estud. Geológicos, 75, 088, https://doi.org/10.3989/egeol.43438.515, 2019.

Fialko, Y. and Pearse, J.: Sombrero Uplift Above the Altiplano-Puna Magma Body: Evidence of a Ballooning Mid-Crustal Diapir, Science (80-.)., 338, 250–252, https://doi.org/10.1126/science.1226358, 2012.

Fídel, L. and Huamaní, A.: Mapa preliminar de amenaza volcánica potencial del Volcán Yucamane, INGEMMET, Boletín N° 26 Ser. C Geodinámica e Ing. Geológica, 165, 2001.

Forte, P., Rodríguez, L., Jácome Paz, M. P., Caballero García, L., Alpízar Segura, Y., Bustos, E., Perales Moya, C., Espinoza,

685   E., Vallejo, S., and Agusto, M.: Volcano monitoring in Latin America: taking a step forward, Volcanica, 4, vii–xxxiii, https://doi.org/10.30909/vol.04.S1.viixxxiii, 2021.

Froger, J.-L., Remy, D., Bonvalot, S., and Legrand, D.: Two scales of inflation at Lastarria-Cordon del Azufre volcanic complex, central Andes, revealed from ASAR-ENVISAT interferometric data, Earth Planet. Sci. Lett., 255, 148–163, https://doi.org/10.1016/j.epsl.2006.12.012, 2007.

690   Gaete, A., Cesca, S., Franco, L., San Martin, J., Cartes, C., and Walter, T. R.: Seismic activity during the 2013–2015 intereruptive phase at Lascar volcano, Chile, Geophys. J. Int., 219, 449–463, https://doi.org/10.1093/gji/ggz297, 2019.

Gałaś, A., Panajew, P., and Cuber, P.: Stratovolcanoes in the Western Cordillera – Polish Scientifi c Expedition to Peru 2003–2012 reconnaissance research, Geotourism/Geoturystyka, 37, 61, https://doi.org/10.7494/geotour.2014.37.61, 2014.

Gardeweg, M., Mpodozis, C., and Clavero, J.: The Ojos del Salado complex: the highest active volcano of the world, Central
695   Andes, Proc. IAVCE, Abstr. Magmat. Divers. Volcanoes their roots, 21, 1998.

Gianni, G. M., Navarrete, C., and Spagnotto, S.: Surface and mantle records reveal an ancient slab tear beneath Gondwana, Sci. Rep., 9, 19774, https://doi.org/10.1038/s41598-019-56335-9, 2019.

Gillespie, R., Magee, J. W., Luly, J. G., Dlugokencky, E., Sparks, R. J., and Wallace, G.: AMS radiocarbon dating in the study of arid environments: Examples from Lake Eyre, South Australia, Palaeogeogr. Palaeoclimatol. Palaeoecol., 84, 333–338,
700   https://doi.org/10.1016/0031-0182(91)90052-S, 1991.

Gonzáles, K., Froger, J., Rivera, M., and Audin, L.: Deformación co-sísmica producida por el sismo Mb=5.4 del 01 de Octubre de 2005 (Carumas-Moquegua), detectada por interferometría radar - InSAR, XIII Congr. Peru. Geolgía. Resúmenes Extendidos Soc. Geológica del Perú, 488–489, 2006.

González-Ferrán, O.: Volcanes de Chile, Instituto Geográfico Militar, 640 pp., 1995.

705   Gottsmann, J., Blundy, J., Henderson, S., Pritchard, M. E., and Sparks, R. S. J.: Thermomechanical modeling of the Altiplano-Puna deformation anomaly: Multiparameter insights into magma mush reorganization, Geosphere, 13, GES01420.1, https://doi.org/10.1130/GES01420.1, 2017.

Grosse, P., Orihashi, Y., Guzmán, S. R., Sumino, H., and Nagao, K.: Eruptive history of Incahuasi, Falso Azufre and El Cóndor Quaternary composite volcanoes, southern Central Andes, Bull. Volcanol., 80, 44, https://doi.org/10.1007/s00445-018-1221-
710   5, 2018.

Grosse, P., Guzmán, S. R., Nauret, F., Orihashi, Y., and Sumino, H.: Central vs. lateral growth and evolution of the < 100 ka Peinado composite volcano, southern Central Volcanic Zone of the Andes, J. Volcanol. Geotherm. Res., 425, https://doi.org/10.1016/j.jvolgeores.2022.107532, 2022.

Guimarães, L., Nieto-Torres, A., Bonadonna, C., and Frischknecht, C.: A New Inclusive Volcanic Risk Ranking, Part 2:
715   Application to Latin America, Front. Earth Sci., 9, 1–24, https://doi.org/10.3389/feart.2021.757742, 2021.

GVP: Global Volcanism Program, Volcanoes World, v. 4.9.2. Venzke, E (ed.). Smithson. Institution., 2013.

GVP: Global Volcanism Program, 2023. Holocene Volcanoes of the World (v. 5.1.1; 17 Aug 2023). Distributed by Smithsonian Institution, compiled by Venzke, E., https://doi.org/10.5479/si.GVP.VOTW5-2023.5.1, 2023a.

GVP: Global Volcanism Program, 2023. Pleistocene Volcanoes of the World (v. 5.1.1; 17 Aug 2023). Distributed by Smithsonian Institution, compiled by Venzke, E., https://doi.org/https://doi.org/10.5479/si.GVP.VOTW5-2023.5.1, 2023b.

Hall, M. L., Samaniego, P., Le Pennec, J. L., and Johnson, J. B.: Ecuadorian Andes volcanism: A review of Late Pliocene to present activity, J. Volcanol. Geotherm. Res., 176, 1–6, https://doi.org/10.1016/j.jvolgeores.2008.06.012, 2008.

Harpel, C. J., de Silva, S., and Salas, G.: The 2 ka Eruption of Misti Volcano, Southern Peru—The Most Recent Plinian Eruption of Arequipa's Iconic Volcano, in: The 2 ka Eruption of Misti Volcano, Southern Peru—The Most Recent Plinian Eruption of Arequipa's Iconic Volcano, Geological Society of America, https://doi.org/10.1130/2011.2484, 2011.

Hayes, G. P., Moore, G. L., Portner, D. E., Hearne, M., Flamme, H., Furtney, M., and Smoczyk, G. M.: Slab2, a comprehensive subduction zone geometry model, Science (80-.)., 362, 58–61, https://doi.org/10.1126/science.aat4723, 2018.

Henderson, S. T. and Pritchard, M. E.: Decadal volcanic deformation in the Central Andes Volcanic Zone revealed by InSAR time series, Geochemistry, Geophys. Geosystems, 14, 1358–1374, https://doi.org/10.1002/ggge.20074, 2013.

Henderson, S. T., Delgado, F., Elliott, J., Pritchard, M. E., and Lundgren, P. R.: Decelerating uplift at Lazufre volcanic center, Central Andes, from A.D. 2010 to 2016, and implications for geodetic models, Geosphere, 13, 1489–1505, https://doi.org/10.1130/GES01441.1, 2017.

Hickey, J., Gottsmann, J., and del Potro, R.: The large-scale surface uplift in the Altiplano-Puna region of Bolivia: A parametric study of source characteristics and crustal rheology using finite element analysis, Geochemistry, Geophys. Geosystems, 14, 540–555, https://doi.org/10.1002/ggge.20057, 2013.

Holtkamp, S. G., Pritchard, M. E., and Lohman, R. B.: Earthquake swarms in South America, Geophys. J. Int., 187, 128–146, https://doi.org/10.1111/j.1365-246X.2011.05137.x, 2011.

IGP: Instituto Geofísico del Perú., Cent. vulcanológico Nac. Volcanes Monit. Perú, 2021.

Inostroza, M., Aguilera, F., Menzies, A., Layana, S., González, C., Ureta, G., Sepúlveda, J., Scheller, S., Böehm, S., Barraza, M., Tagle, R., and Patzschke, M.: Deposition of metals and metalloids in the fumarolic fields of Guallatiri and Lastarria volcanoes, northern Chile, J. Volcanol. Geotherm. Res., 393, 106803, https://doi.org/10.1016/j.jvolgeores.2020.106803, 2020a.

Inostroza, M., Tassi, F., Aguilera, F., Sepúlveda, J. P., Capecchiacci, F., Venturi, S., and Capasso, G.: Geochemistry of gas and water discharge from the magmatic-hydrothermal system of Guallatiri volcano, northern Chile, Bull. Volcanol., 82, 57, https://doi.org/10.1007/s00445-020-01396-2, 2020b.

Jaillard, E., Hérail, G., Monfret, T., Diaz-Martinez, E., Baby, P., Lavenu, A., and Dumont, J. F.: Tectonic evolution of the Andes of Ecuador, Peru, Bolivia and Northernmost Chile. In Tectonic evolution of South America (Cordani, U.; Milani, E.; Thomaz Filho, A.; Campos; D.; editors), Tecton. Evol. South Am., 31, 481–559, 2000.

James, D. E.: Andean crustal and upper mantle structure, J. Geophys. Res., 76, 3246–3271, https://doi.org/10.1029/JB076i014p03246, 1971.

Jay, J. A., Pritchard, M. E., West, M. E., Christensen, D., Haney, M., Minaya, E., Sunagua, M., McNutt, S. R., and Zabala, M.: Shallow seismicity, triggered seismicity, and ambient noise tomography at the long-dormant Uturuncu Volcano, Bolivia,

Bull. Volcanol., 74, 817–837, https://doi.org/10.1007/s00445-011-0568-7, 2012.

Jay, J. A., Welch, M., Pritchard, M. E., Mares, P. J., Mnich, M. E., Melkonian, A. K., Aguilera, F., Naranjo, J. A., Sunagua,

755   M., and Clavero, J.: Volcanic hotspots of the central and southern Andes as seen from space by ASTER and MODVOLC between the years 2000 and 2010, Geol. Soc. London, Spec. Publ., 380, 161–185, https://doi.org/10.1144/SP380.1, 2013.

Jay, J. A., Delgado, F. J., Torres, J. L., Pritchard, M. E., Macedo, O., and Aguilar, V.: Deformation and seismicity near Sabancaya volcano, southern Peru, from 2002 to 2015, Geophys. Res. Lett., 42, 2780–2788, https://doi.org/10.1002/2015GL063589, 2015.

760   Jordan, T., Isacks, B., Allmendinger, R., Brewer, J., Ramos, V., and Ando, C.: Andean tectonics related to geometry of subducted Nazca plate, Geol. Soc. Am. Bull., 94, 341, https://doi.org/10.1130/0016-7606(1983)94<341:ATRTGO>2.0.CO;2, 1983.

Kay, S. M. and Coira, B. L.: Shallowing and steepening subduction zones, continental lithospheric loss, magmatism, and crustal flow under the Central Andean Altiplano-Puna Plateau, Mem. Geol. Soc. Am., 204, 229–259,
765   https://doi.org/10.1130/2009.1204(11), 2009.

Lamberti, M. C., Chiodi, A., Agusto, M., Filipovich, R., Massenzio, A., Báez, W., Tassi, F., and Vaselli, O.: Carbon dioxide diffuse degassing as a tool for computing the thermal energy release at Cerro Blanco Geothermal System, Southern Puna (NW Argentina), J. South Am. Earth Sci., 105, 102833, https://doi.org/10.1016/j.jsames.2020.102833, 2021.

Lara, L. ., Orozco, G., Amigo, A., and Silva, C.: Peligros Volcánicos de Chile. Servicio Nacional de Geología y Minería, Carta
770   Geológica de Chile, Serie Geología Ambiental, 0–24, 1 mapa escala 1:2.000.000, 2011.

Liu, F., Elliott, J., Ebmeier, S., Craig, T., Hooper, A., Novoa, C., and Delgado, F.: Unrest Detected at Socompa Volcano, Northern Chile, from Geodetic Observations, AGU Fall Meet. Abstr., G46A-02, 2022.

Liu, F., Elliott, J. R., Ebmeier, S. K., Craig, T. J., Hooper, A., Novoa Lizama, C., and Delgado, F.: First Onset of Unrest Captured at Socompa: A Recent Geodetic Survey at Central Andean Volcanoes in Northern Chile, Geophys. Res. Lett., 50,
775   https://doi.org/10.1029/2022GL102480, 2023.

Loyola, R., Figueroa, V., Núñez, L., Vasquez, M., Espíndola, C., Valenzuela, M., and Prieto, M.: The Volcanic Landscapes of the Ancient Hunter-Gatherers of the Atacama Desert Through Their Lithic Remains, Front. Earth Sci., 10, 1–22, https://doi.org/10.3389/feart.2022.897307, 2022.

Macedo, O., Taipe, E., Del Carpio, J., Ticona, J., Ramos, D., Puma, N., Aguilar, V., Machacca, R., Torres, J., Cueva, K., Cruz,
780   J., Lazarte, I., Centeno, R., Miranda, R., Álvarez, Y., Masias, P., Vilca, J., Apaza, F., Chijcheapaza, R., Calderón, J., Cáceres, J., and Vela, J.: Evaluación del Riesgo Volcánico en el Sur del Perú, situación actual de la vigilancia actual y requerimientos de monitoreo en el futuro, Arequipa, 2016.

Mariño, J., Samaniego, P., Manrique, N., Valderrama, P., and Macedo, L.: Geología y Mapa de Peligros del Complejo Volcánico Tutupaca, INGEMMET, Boletín Ser. C Geodinámica e Ing. Geológica N° 66, 168, 2019.

785   Matthews, S. J., Gardeweg, M. C., and Sparks, R. S. J.: The 1984 to 1996 cyclic activity of Lascar Volcano, northern Chile: cycles of dome growth, dome subsidence, degassing and explosive eruptions, Bull. Volcanol., 59, 72–82,

https://doi.org/10.1007/s004450050176, 1997.

Van der Meijde, M., Julià, J., and Assumpção, M.: Gravity derived Moho for South America, Tectonophysics, 609, 456–467, https://doi.org/10.1016/j.tecto.2013.03.023, 2013.

790   Méndez-Fajury, R. A.: Catálogo de Volcanes Activos en Colombia, Boletín Geológico INGEOMINAS, 30, 1–75, 1989.

Morales Rivera, A. M., Amelung, F., and Mothes, P.: Volcano deformation survey over the Northern and Central Andes with ALOS InSAR time series, Geochemistry, Geophys. Geosystems, 17, 2869–2883, https://doi.org/10.1002/2016GC006393, 2016.

Mulcahy, P., Chen, C., Kay, S. M., Brown, L. D., Alvarado, P. M., Sandvol, E. A., Heit, B., and Yuan, X.: The Southern Puna 795   seismic experiment: shape of the subducting Nazca Plate, areas of concentrated mantle and crustal earthquakes, and crustal focal mechanisms, Am. Geophys. Union, Fall Meet. 2010, Abstr. id. T11A-2050, 1, 2010.

Naranjo, J. A.: Sulphur flows at Lastarria volcano in the North Chilean Andes, Nature, 313, 778–780, https://doi.org/10.1038/313778a0, 1985.

Nieto-Torres, A., Guimarães, L. F., Bonadonna, C., and Frischknecht, C.: A New Inclusive Volcanic Risk Ranking, Part 1: 800   Methodology, Front. Earth Sci., 9, 1–22, https://doi.org/10.3389/feart.2021.697451, 2021.

Nieto, A.: Volcanic Risk Ranking for México and Central América, Spec. Certif. Assess. Manag. Geol. Clim. Relat. risk, CERG-C 2019, 42, 2020.

OVI: Observatorio Vulcanológico del INGEMMET, Inst. Geol. Min. y Metal., 2021.

Pavez, A., Remy, D., Bonvalot, S., Diament, M., Gabalda, G., Froger, J.-L., Julien, P., Legrand, D., and Moisset, D.: Insight 805   into ground deformations at Lascar volcano (Chile) from SAR interferometry, photogrammetry and GPS data: Implications on volcano dynamics and future space monitoring, Remote Sens. Environ., 100, 307–320, https://doi.org/10.1016/j.rse.2005.10.013, 2006.

Pavez, C., Comte, D., Gutiérrez, F., and Gaytán, D.: Analysis of the magmatic – Hydrothermal volcanic field of Tacora Volcano, northern Chile using travel time tomography, J. South Am. Earth Sci., 94, 102247, 810   https://doi.org/10.1016/j.jsames.2019.102247, 2019.

Petit-Breuilh Sepúlveda, M.: Volcanes fronterizos en América Latina y la importancia de los comités de frontera en casos de desastre: Chile y Argentina en el siglo XX., in: Clima, desastres y convulsiones sociales en España e Hispanoamérica, siglos XVII-XX., 2016.

Pieri, D. and Abrams, M.: ASTER watches the world's volcanoes: a new paradigm for volcanological observations from orbit, 815   J. Volcanol. Geotherm. Res., 135, 13–28, https://doi.org/10.1016/j.jvolgeores.2003.12.018, 2004.

Pilger, R. H.: Cenozoic plate kinematics, subduction and magmatism: South American Andes, J. Geol. Soc. London., 141, 793–802, https://doi.org/10.1144/gsjgs.141.5.0793, 1984.

Pritchard, M. and Simons, M.: An InSAR-based survey of volcanic deformation in the central Andes, Geochemistry, Geophys. Geosystems, 5, 1–42, https://doi.org/10.1029/2003GC000610, 2004.

820   Pritchard, M. E. and Simons, M.: A satellite geodetic survey of large-scale deformation of volcanic centres in the central

33

Andes, Nature, 418, 167–171, https://doi.org/10.1038/nature00872, 2002.

Pritchard, M. E., Henderson, S. T., Jay, J. A., Soler, V., Krzesni, D. A., Button, N. E., Welch, M. D., Semple, A. G., Glass, B., Sunagua, M., Minaya, E., Amigo, A., and Clavero, J.: Reconnaissance earthquake studies at nine volcanic areas of the central Andes with coincident satellite thermal and InSAR observations, J. Volcanol. Geotherm. Res., 280, 90–103,

825   https://doi.org/10.1016/j.jvolgeores.2014.05.004, 2014.

Pritchard, M. E., de Silva, S. L., Michelfelder, G., Zandt, G., McNutt, S. R., Gottsmann, J., West, M. E., Blundy, J., Christensen, D. H., Finnegan, N. J., Minaya, E., Sparks, R. S. J., Sunagua, M., Unsworth, M. J., Alvizuri, C., Comeau, M. J., del Potro, R., Díaz, D., Diez, M., Farrell, A., Henderson, S. T., Jay, J. A., Lopez, T., Legrand, D., Naranjo, J. A., McFarlin, H., Muir, D., Perkins, J. P., Spica, Z., Wilder, A., and Ward, K. M.: Synthesis: PLUTONS: Investigating the relationship

830   between pluton growth and volcanism in the Central Andes, Geosphere, 14, 954–982, https://doi.org/10.1130/GES01578.1, 2018.

Ramos Chocobar, S. and Tironi, M.: An Inside Sun: Lickanantay Volcanology in the Salar de Atacama, Front. Earth Sci., 10, 1–11, https://doi.org/10.3389/feart.2022.909967, 2022.

Ramos, D.: Evaluación de la Actividad de los Volcanes Misti y Coropuna, INGEMMET, Inf. Técnico N°A69, 27, 2019.

835   Ramos, V. A. and Aleman, A.: Tectonic evolution of the Andes, 31st Int. Geol. Congr., 635–685, 2000.

REAV Parinacota: Reporte Especial de Actividad Volcánica, Región de Arica y Parinacota, Volcán Parinacota, Serv. Nac. Geol. y Minería, 2, 2020.

Reyes-Hardy, M.-P., Di Maio, L. S., Dominguez, L., Frischknecht, C., Biasse, S., Guimarães, L., Nieto-Torres, A., Elissondo, M., Pedreros, G., Aguilar, R., Amigo, Á., Garcia, S., Forte, P., and Bonadonna, C.: Active and potentially active volcanoes of

840   the Central Volcanic Zone of the Andes (CVZA), Arch. Ouvert. UNIGE, 123, https://doi.org/10.13097/archive-ouverte/unige, 2023.

Rivera, M., Thouret, J.-C., Mariño, J., Berolatti, R., and Fuentes, J.: Characteristics and management of the 2006–2008 volcanic crisis at the Ubinas volcano (Peru), J. Volcanol. Geotherm. Res., 198, 19–34, https://doi.org/10.1016/j.jvolgeores.2010.07.020, 2010.

845   Rivera, M., Cueva, K., Vela, J., Soncco, Y., Manrique, N., Le Pennec, J.-L., and Samaniego, P.: Mapa Geológico del Volcán Sara Sara (Ayacucho) Escala 1:25,000, 1, 1 mapa, 2020.

Robidoux, P., Rizzo, A. L., Aguilera, F., Aiuppa, A., Artale, M., Liuzzo, M., Nazzari, M., and Zummo, F.: Petrological and noble gas features of Lascar and Lastarria volcanoes (Chile): Inferences on plumbing systems and mantle characteristics, Lithos, 370–371, 105615, https://doi.org/10.1016/j.lithos.2020.105615, 2020.

850   Romero, H. and Albornoz, C.: Erupciones volcánicas, en Chile, Rev. Retratos la Esc. Brasília, 7, 513–527, 2013.

Ruch, J. and Walter, T. R.: Relationship between the InSAR-measured uplift, the structural framework, and the present-day stress field at Lazufre volcanic area, central Andes, Tectonophysics, 492, 133–140, https://doi.org/10.1016/j.tecto.2010.06.003, 2010.

Ruch, J., Anderssohn, J., Walter, T. R., and Motagh, M.: Caldera-scale inflation of the Lazufre volcanic area, South America:

855 Evidence from InSAR, J. Volcanol. Geotherm. Res., 174, 337–344, https://doi.org/10.1016/j.jvolgeores.2008.03.009, 2008.

Ruch, J., Manconi, A., Zeni, G., Solaro, G., Pepe, A., Shirzaei, M., Walter, T. R., and Lanari, R.: Stress transfer in the Lazufre volcanic area, central Andes, Geophys. Res. Lett., 36, L22303, https://doi.org/10.1029/2009GL041276, 2009.

Samaniego, P., Rivera, M., Mariño, J., Guillou, H., Liorzou, C., Zerathe, S., Delgado, R., Valderrama, P., and Scao, V.: The eruptive chronology of the Ampato–Sabancaya volcanic complex (Southern Peru), J. Volcanol. Geotherm. Res., 323, 110–

860 128, https://doi.org/10.1016/j.jvolgeores.2016.04.038, 2016.

Sandri, L., Thouret, J.-C., Constantinescu, R., Biass, S., and Tonini, R.: Long-term multi-hazard assessment for El Misti volcano (Peru), Bull. Volcanol., 76, 771, https://doi.org/10.1007/s00445-013-0771-9, 2014.

Schoenbohm, L. M. and Carrapa, B.: Miocene–Pliocene shortening, extension, and mafic magmatism support small-scale lithospheric foundering in the central Andes, NW Argentina, in: Geodynamics of a Cordilleran Orogenic System: The Central

865 Andes of Argentina and Northern Chile, vol. 212, Geological Society of America, 167–180, https://doi.org/10.1130/2015.1212(09), 2015.

Seggiaro, R. and Apaza, F.: Geología del proyecto geotérmico Socompa, Serv. Geológico Min. Argentino. Inst. Geol. y Recur. Miner. Buenos Aires, 26, 2018.

Sempere, T., Hérail, G., Oller, J., and Bonhomme, M. G.: Late Oligocene-early Miocene major tectonic crisis and related

870 basins in Bolivia, Geology, 18, 946, https://doi.org/10.1130/0091-7613(1990)018<0946:LOEMMT>2.3.CO;2, 1990.

SERNAGEOMIN: Servicio Nacional de Geología y Minería., Red Nac. Vigil. volcánica. Volcanes Act. y Monit. por cada región del país, Chile., 2021.

SERNAGEOMIN: Ranking de riesgo específico para volcanes activos de Chile 2023, 2023.

De Silva, S. and Francis, P.: Volcanoes of the Central Andes, Springer Verlag, Berlín, 216 p., Berlin, 216 pp., 1991.

875 Sparks, R. S. J., Folkes, C. B., Humphreys, M. C. S., Barfod, D. N., Clavero, J., Sunagua, M. C., McNutt, S. R., and Pritchard, M. E.: Uturuncu volcano, Bolivia: Volcanic unrest due to mid-crustal magma intrusion, Am. J. Sci., 308, 727–769, https://doi.org/10.2475/06.2008.01, 2008.

Spica, Z., Legrand, D., Mendoza, A. I., Dahn, T., Walter, T., Heimann, S., Froger, J. L., and Rémy, D.: Analysis of surface waves extracted from seismic noise for the Lastarria volcanic zone, Chile., Cities Volcanoes 7, Colima, México., 2012.

880 Stern, C.: Active Andean volcanism: its geologic and tectonic setting, Rev. geológica Chile, 31, 106–123, https://doi.org/10.4067/S0716-02082004000200001, 2004.

Szakács, A.: Redefining active volcanoes: a discussion, Bull. Volcanol., 56, 321–325, https://doi.org/10.1007/BF00326458, 1994.

Tassi, F., Aguilera, F., Vaselli, O., Medina, E., Tedesco, D., Delgado Huertas, A., Poreda, R., and Kojima, S.: The magmatic-

885 and hydrothermal-dominated fumarolic system at the Active Crater of Lascar volcano, northern Chile, Bull. Volcanol., 71, 171–183, https://doi.org/10.1007/s00445-008-0216-z, 2009.

Tassi, F., Aguilera, F., Vaselli, O., Darrah, T., and Medina, E.: Gas discharges from four remote volcanoes in northern Chile (Putana, Olca, Irruputuncu and Alitar): a geochemical survey, Ann. Geophys., 54, 121–136, https://doi.org/10.4401/ag-5173,

2011.

890 Thorpe, R. S., Francis, P. W., and O'Callaghan, L. J.: Relative roles of source composition, fractional crystallization and crustal contamination in the petrogenesis of Andean volcanic rocks, Philos. Trans. R. Soc. London. Ser. A, Math. Phys. Sci., 310, 675–692, https://doi.org/10.1098/rsta.1984.0014, 1984.

Thouret, J., Finizola, A., Fornari, M., Suni, J., and Frechen, M.: Geology of El Misti volcano near the city of Arequipa , Peru, Geol. Soc. Am. Bull., 113, 1593–1610, https://doi.org/10.1130/0016-7606(2001)1132.0.CO;2, 2001.

895 Tilling, R. I.: Volcanism and associated hazards: the Andean perspective, Adv. Geosci., 22, 125–137, https://doi.org/10.5194/adgeo-22-125-2009, 2009.

Vélez, M. ., Bustos, E., Euillades, L., Blanco, M., López, J. F. S., Barbero, I., Berrocoso, M., Gil Martinez, A., and Viramonte, J. G.: Ground deformation at the Cerro Blanco caldera: A case of subsidence at the Central Andes BackArc, J. South Am. Earth Sci., 106, 102941, https://doi.org/10.1016/j.jsames.2020.102941, 2021.

900 Viramonte, J., Godoy, S., Arnosio, M., Becchio, R., and Poodts, M.: El campo geotermal de la caldera del cerro Blanco: utilización de imágenes aster, Proc. Geol. Congr. Buenos Aires, Asoc. Geológica Argentina. La Plata, Argentina., 2, 505–512, 2005.

Viramonte, J. G., Galliski, M. A., Araña Saavedra, V., Aparicio, A., Garcia Cacho, L., and Martín Escorza, C.: El finivolcanismo básico de la depresión de Arizaro, provincia de Salta., IX Congr. Geológico Argentino Actas III, 234–251, 905 1984.

Walker, B. A., Klemetti, E. W., Grunder, A. L., Dilles, J. H., Tepley, F. J., and Giles, D.: Crystal reaming during the assembly, maturation, and waning of an eleven-million-year crustal magma cycle: thermobarometry of the Aucanquilcha Volcanic Cluster, Contrib. to Mineral. Petrol., 165, 663–682, https://doi.org/10.1007/s00410-012-0829-2, 2013.